ENVIRONMENTAL SALINITY MODULATES THE EFFECTS OF ELEVATED CO_2 LEVELS ON JUVENILE HARD SHELL CLAMS, *MERCENARIA MERCENARIA*

Gary H. Dickinson[1,2a], Omera B. Matoo[3a], Robert T. Tourek[1], Inna M. Sokolova[3*], Elia Beniash[1*]

[1] Department of Oral Biology, University of Pittsburgh, 589 Salk Hall, 3501 Terrace Street, Pittsburgh, PA 15261, USA

[2] Department of Biology, The College of New Jersey, 2000 Pennington Road, Ewing, NJ 08628, USA

[3] Department of Biology, University of North Carolina at Charlotte, 9201 University City Blvd., Charlotte, NC 28223, USA

[a]These authors contributed equally to the work

[*]Corresponding authors:

Inna Sokolova,
isokolov@uncc.edu
Department of Biology
9201 University City Blvd.
Charlotte, NC 28223, USA

Elia Beniash
ebeniash@pitt.edu
Department of Oral Biology,
University of Pittsburgh,
589 Salk Hall, 3501 Terrace Street,
Pittsburgh, PA 15261, USA

Running title: Salinity and elevated CO_2 affect juvenile clams

Key words: Ocean acidification, salinity, estuary, standard metabolic rate, biomineralization, shell properties, mollusks

ABSTRACT. Ocean acidification due to increasing atmospheric CO_2 concentrations results in a decrease in seawater pH and shifts in the carbonate chemistry that can negatively affect marine organisms. Marine bivalves such as the hard shell clams *Mercenaria mercenaria* serve as ecosystem engineers in estuaries and coastal zones of the western Atlantic and, as for many marine calcifiers, are sensitive to the impacts of ocean acidification. In estuaries, the effects of ocean acidification can be exacerbated by low buffering capacity of brackish waters, acidic inputs from freshwaters and land, and/or the negative effects of salinity on organisms' physiology. We determined the interactive effects of 21 weeks of exposure to different levels of CO_2 (~395, 800 and 1500 µatm corresponding to pH of 8.2, 8.1 and 7.7 respectively) and salinity (32 vs. 16) on biomineralization, shell properties and energy metabolism of juveniles of the hard shell clam *Mercenaria mercenaria*. Low salinity had profound effects on survival, energy metabolism and biomineralization of hard shell clams and modulated their responses to elevated P_{CO2}. Negative effects of low salinity in juvenile clams were mostly due to the strongly elevated basal energy demand indicating energy deficiency that led to reduced growth, elevated mortality and impaired shell maintenance (evidenced by the extensive damage to the periostracum). The effects of elevated P_{CO2} on physiology and biomineralization of hard shell clams were more complex. Elevated P_{CO2} (~800-1500 µatm) had no significant effects on standard metabolic rates (indicative of the basal energy demand), but affected growth and shell mechanical properties in juvenile clams. Moderate hypercapnia (~ 800 µatm P_{CO2}) increased shell and tissue growth and reduced mortality of juvenile clams in high salinity exposures; however, these effects were abolished under the low salinity conditions or at high P_{CO2} (~1500 µatm). Mechanical properties of the shell (measured as microhardness and fracture toughness of the shells) were negatively affected by elevated CO_2 alone or in combination with low salinity, which may have important implications for protection against predators or environmental stressors. Our data indicate that environmental salinity can strongly modulate responses to ocean acidification in hard shell clams and thus should be taken into account when predicting the effects of ocean acidification on estuarine bivalves.

INTRODUCTION

Current models of global change predict a rise in the atmospheric carbon dioxide (CO_2) levels from the current value of ~380-400 µatm to 730-1020 µatm by the year 2100 and 1500-2000 µatm in the next 300 years (Doney *et al.*, 2009; Waldbusser *et al.*, 2011). About 30% of the anthropogenically released CO_2 is absorbed by the ocean resulting in ocean acidification, which involves a drop in seawater pH, shifts in the inorganic carbon speciation and a decrease in saturation of calcium carbonate ($CaCO_3$) minerals and can strongly affect marine organisms (Kleypas *et al.*, 2006; Pörtner, 2008a; Przeslawski *et al.*, 2008; Cooley and Doney, 2009). Estuarine and coastal habitats, the ocean's hotspots for biological diversity and productivity, may be especially vulnerable to ocean acidification. They often receive acidic inputs from freshwater and land run-off, upwelling of the CO_2-enriched acidified waters as well as from biological CO_2 production, leading to large fluctuations in pH and carbonate chemistry (Mook and Koene, 1975; Cai and Wang, 1998; Thomsen *et al.*, 2010; Amaral *et al.*, 2011). Moreover, the buffering capacity of estuarine waters is considerably lower than that of the open ocean (Mook and Koene, 1975; Cai and Wang, 1998). An increase in atmospheric CO_2 levels can exacerbate acidification of estuarine habitats, and long-term pH data show that some estuaries have become more acidic in the past 50 years with the rate of acidification closely tracking atmospheric CO_2 (Najjar *et al.*, 2010; Waldbusser *et al.*, 2011).

Bivalve mollusks play a prominent ecological role as ecosystem engineers and key foundation species in estuarine and coastal ecosystems around the world (Gutiérrez *et al.*, 2003; Kochmann *et al.*, 2008). Mollusks belong to a broad group of marine organisms called marine calcifiers (i.e. organisms that build their skeleton from $CaCO_3$) that are among the most sensitive groups of

organisms to ocean acidification (Kleypas *et al.*, 2006; Dupont *et al.*, 2010; Kroeker *et al.*, 2010). Ocean acidification strongly affects biomineralization of calcifiers due to the decrease in pH and saturation of $CaCO_3$ minerals, which slows deposition rates and increases solubility of $CaCO_3$ (Gazeau *et al.*, 2007; Byrne *et al.*, 2011). The effects of elevated CO_2 on molluscan biomineralization can be very complex depending on the shell structure, mineralogy and biological factors involved in the control of shell formation (Addadi *et al.*, 2006; Stanley, 2006; Ries *et al.*, 2009; Kroeker *et al.*, 2010). Elevated CO_2 levels can have systemic effects on the physiology of marine mollusks that extend beyond calcification, affecting their extra- and intracellular pH, enzyme activity, protein stability and rates of energy metabolism (Pörtner, 2008b; Lannig *et al.*, 2010; Tomanek *et al.*, 2011; Pörtner, 2012). These changes may directly affect the organism's performance and fitness as well as indirectly influence biomineralization via impacts on physiological functions such as activity of biomineralization enzymes and energy metabolism.

In estuaries, ocean acidification can be compounded by other environmental parameters (such as temperature, salinity and anthropogenic pollution) that can modulate the effects of elevated CO_2 (Lannig *et al.*, 2010; Dickinson *et al.*, 2012; Nikinmaa, 2013). Among these parameters, salinity is likely to play a key role due to its direct effect on seawater chemistry and buffering capacity as well as on the physiology of estuarine inhabitants. In osmoconforming animals, such as marine mollusks, reduced salinity has a strong impact on physiology leading to changes in the cell volume, extra- and intracellular osmotic pressure, altering energy metabolism and enzyme activities, and affecting the rates of protein synthesis and turnover (Berger, 1986; Prosser, 1991; Berger and Kharazova, 1997). Earlier studies also showed that low salinity can exacerbate negative effects of

elevated CO_2 levels on growth, energy balance and biomineralization of a common estuarine bivalve, the eastern oyster *Crassostrea virginica* (Dickinson *et al.*, 2012). However, the interactive effects of salinity and elevated CO_2 on marine organisms are not yet fully understood and require further investigation.

The aim of this study was to characterize the interactive effects of two common environmental factors – elevated CO_2 and low salinity – on biomineralization, shell properties and energy metabolism of a common estuarine bivalve, the hard shell clam *Mercenaria mercenaria*. *M. mercenaria* is an ecosystem engineer in temperate estuaries and coastal zones of the Atlantic affecting sediment structure and playing an important role in trophic interactions. Hard shell clams are also economically important, with annual worldwide harvests ranging from 30,000 to 70,000 tons (Food and Agriculture Organization of the United Nations (FAO), Aquaculture and Fishery Statistics at http://www.fao.org). Shells of hard shell clams are made of aragonite, a more soluble polymorph of $CaCO_3$ than calcite, and consist of an outer thick prismatic and inner cross-lamellar layer (Kraeuter and Castagna, 2001). This relatively simple shell mineralogy makes clams a useful model species for studying the effects of ocean acidification and salinity on biomineralization and shell properties. We tested the hypothesis that low salinity (such as commonly occurs in the estuarine habitats of hard shell clams) will exacerbate the effects of ocean acidification resulting in reduced growth and biomineralization and elevated basal energy metabolism that may decrease the amount of energy invested into growth and shell formation.

MATERIALS AND METHODS

Chemicals. Chemicals and enzymes were purchased from Sigma Aldrich (St. Louis, MO, USA), Roche (Indianapolis, IN, USA) or Fisher Scientific (Pittsburg, PA, USA) unless otherwise stated, and were of analytical grade or higher.

Experimental design. The effects of two factors, P_{CO2} and salinity, were tested in a full factorial design. Three P_{CO2} levels, ~395 µatm (normocapnia, pH_{NBS} 8.25-8.26), ~800 µatm (moderate hypercapnia, pH_{NBS} 8.15-8.16) and ~1500 µatm (extreme hypercapnia, pH_{NBS} 7.74-7.77) were assessed at a salinity of 32 (high salinity) or 16 (low salinity), yielding six treatment groups. P_{CO2} levels were chosen to be representative of the present-day P_{CO2} (~395 µatm), atmospheric P_{CO2} predicted by moderate IPCC scenarios (IPCC) for the year 2100 (~800 µatm CO_2), and a P_{CO2} projection for the year 2250 (~1500 µatm). The two selected salinity conditions were within the environmentally relevant range for *M. mercenaria*. Clams were randomly assigned to one of the six treatment groups and exposed for a total of 21 weeks. The group exposed to a salinity of 32 and ~395 µatm P_{CO2} was considered control. Non-reproductive juveniles were used in this study in order to avoid complications due to the varying energy demands of reproducing organisms in different stages of their reproductive cycle. The salinity and CO_2 levels used in this study are within the range currently found in the estuaries of the southeastern United States where the clams were collected (Burnett, 1997; Ringwood and Keppler, 2002; McElhany and Busch, 2012). It is worth noting that clams can periodically experience much stronger acidification in their present-day habitats (with pH dropping below 7.0) than those used in the present study (Ringwood and Keppler, 2002); however, such extreme events usually only last from a few hours

to a few days. The long-term exposures such as used in the present study are more representative of the future ocean acidification scenarios.

Animal collection and maintenance. Juvenile *Mercenaria mercenaria* (8 weeks post metamorphosis) were purchased from a commercial supplier (Grant's Oyster House, NC, USA) and shipped overnight to the University of North Carolina at Charlotte. Clams were acclimated for 7 days in plastic trays (28 cm x 18 cm x 12 cm) each containing 5 l of artificial seawater (ASW: Instant Ocean®, Kent Marine, Acworth, USA) at 20±1°C and salinity of 32±1 bubbled with ambient air (normocapnia, P_{CO2} ~ 395 µatm). Animals were then randomly assigned to a high or low salinity treatment. Salinity was maintained at 32 for the high salinity group and was reduced gradually by 3 units per day until a salinity of 16 was reached.

Once the target salinity was reached, clams were further divided into groups assigned to different P_{CO2} treatments. Target P_{CO2} values were reached by bubbling seawater with gas mixtures containing different CO_2 concentrations. For normocapnic treatment (P_{CO2} ~395 µatm), the tanks were bubbled with the ambient air. For moderate and extreme hypercapnia (~800 and 1500 µatm P_{CO2}, respectively), ambient air was mixed with 100% CO_2 (Roberts Oxygen, NC, USA) in a fixed proportion using precision mass flow controllers (Cole-Parmer, IL, USA) and bubbled into the trays. Air-CO_2 mixture flow rate was set up to maintain the respective systems at a steady-state pH during the exposures. Two replicate trays were used for each species and treatment condition with approximately 400-500 animals per tray. Water temperature was maintained at 20±1°C throughout the duration of the experiment. Salinity and temperature was measured with an YSI30 salinity, temperature, and conductivity meter (YSI Inc., Yellow Springs, OH, USA). Salinity was determined on the practical salinity scale and reported in PSU (practical salinity units). Water was

changed every other day using ASW pre-equilibrated with the respective gas mixtures. Animals were fed *ad libitum* on alternative days with 2 ml per tray of commercial algal mixture containing *Isochrysis* spp., *Pavlova* spp., *Thalassoisira weissflogii,* and *Tetraselmis* spp. with 5-20 µm cells (Shellfish Diet 1800, Reed Mariculture Inc.). Mortality was checked weekly.

Seawater chemistry. Seawater chemistry parameters were determined in all experimental treatments (Table 1) as described elsewhere (Beniash *et al.*, 2010). Water temperature, salinity and pH in the exposure trays was monitored throughout the course of the experiment, and water samples were collected periodically in air-tight containers, poisoned with mercuric chloride and stored at +4°C until further analysis. pH was measured using a pH electrode (pH meter Model 1671, Jenco Instruments, San Diego, CA, USA) calibrated with National Institute of Standards and Technology standard pH buffer solutions (National Bureau of Standards, NBS standards, Fisher Scientific). Total dissolved inorganic carbon (DIC) was measured by the Nutrient Analytical Services (Chesapeake Biological Laboratory, Solomons, MD, USA). Seawater carbonate chemistry parameters (P_{CO2}, total alkalinity, and the saturation state (Ω) for calcite and aragonite) were calculated using CO2SYS software (Lewis and Wallace, 1998) using barometric pressure values, as well as DIC, pH, temperature and salinity values for the respective samples. For calculations, we used NBS scale for seawater pH, constants from Millero et al. (Millero et al., 2006 cited after Lewis and Wallace, 1998), KSO_4^- constant from Dickson (Dickson, 1990), and concentrations of silicate and phosphate for Instant Ocean® seawater (silicate: 0.17 and 0.085 µmol kg^{-1} at salinities of 32 and 16, respectively, and phosphate: 0.04 and 0.02 µmol kg^{-1} at salinities of 32 and 16, respectively).

Shell mass and tissue mass. After 16 and 21 weeks exposure, a subset of clams from each treatment group was stored in 70% ethanol and shipped to the University of Pittsburgh for mass measurements, mechanical testing, and structural and mineralogical analyses. Upon receipt, clams were manually inspected and any clams with visible signs of shell damage were discarded.

For dry mass measurements, 11 – 40 animals (depending on availability) were randomly selected from each treatment group. Individual clams were dried in a vacuum oven at 45°C, 27" Hg for at least 15 days to achieve constant mass and weighed individually on a microbalance (Metler-Toledo XP 26, Columbus, OH) with precision of 0.01 mg or better. Once the total masses of individual clams had been determined, each clam was incubated in 500 µl sodium hypochlorite (NaOCl; commercial Clorox diluted to obtain 2% v/v NaOCl and filtered through a 0.2 µm filter) at room temperature (RT) for 10 days, with three changes of NaOCl solution to ensure complete removal of soft tissues. NaOCl-treated shells of individual clams were rinsed three times in deionized water, dried in air (24 h at RT) and a vacuum oven (24 h at 45°C), and weighed on a microbalance to obtain the shell mass. Tissue dry mass was determined as the difference between the total dry mass of the clam and the dry mass of the shell.

Mechanical properties of the shells. Mechanical properties, structure and mineralogy of the shells were analyzed in the whole shells of experimental clams (i.e. including new growth and pre-existing shell) because the region of new shell growth was too small for the analyses. Therefore, results of these analyses should be interpreted as encompassing both the newly deposited shell material and changes in the existing shell due to the differences in the seawater chemistry.

Micromechanical testing was conducted on left valves of the NaOCl-treated shells of clams that had been exposed to experimental conditions for 21 weeks. For each treatment group, 7 shells were tested. Clams were selected for analysis that approximated the mean mass of all clams when all treatments were combined (3.06 mg). Left shell valves were mounted in epoxy resin (Epofix, EMS Hatfield, PA) in a flat silicone embedding mold (EMS, Hatfield, PA) and polymerized for 24 hours at RT. Embedded shells were cut longitudinally, transecting the anterior apical tip to the most posterior distal edge using a slow-speed water-cooled diamond saw (IsoMet, Buehler, Lake Bluff, Il). A second cut was made parallel to the first one to produce a 3 mm thick section, as described previously (Dickinson *et al.*, 2012). Sections were ground and polished with Metadi diamond suspensions at 6, 1, and 0.25 µm particle size on a grinder-polisher (MiniMet 1000, Buehler, Lake Bluff, IL). Grinding and polishing was conducted using a saturated $CaCO_3$ solution (pH 8.1) prepared by mixing calcium and carbonate salts at very high concentrations and letting the mineral precipitate over several hours. The mixture was centrifuged and the supernatant used to polish the samples. No etching of the shell samples was observed during grinding or polishing.

Vickers microhardness tests were conducted using a microindentation hardness tester (IndentaMet 1104, Buehler, Lake Bluff, IL) on polished shells at 0.245 N load and 5 s dwelling time. Indents were made within the middle layer of the shell (cross lamellar homogenous layer) in a region equidistant from the apical anterior tip and the most distal posterior edge. Five to seven indentations per shell were made at least 30 µm away from the shell edges and from other indents. Vickers hardness numbers (VHN) were averaged for each shell sample. Digital photographs were taken before and immediately after each indentation. This enabled quantification of the longest crack produced by each indent, which was measured using Photoshop

227 software (Ver. 4.0, Adobe, San Jose, CA) as the radius of a circle radiating from the center of the
228 indent enclosing all visible cracks. The crack radius for a shell sample was obtained by averaging
229 the crack radii for all indents on that sample, expressed in μm.

230 Hardness and crack radius measurements were used to calculate fracture toughness (K_c) for each
231 sample as described elsewhere (Anstis *et al.*, 1981; Baldassarri *et al.*, 2008):

232 $K_C = 0.0154 \times (E/H)^{1/2} \times (P/C^{1.5})$

233 where 0.0154 is a calibration constant, E is an elastic modulus (empirically determined for *M.*
234 *mercenaria* as 66 GPa: Currey and Taylor, 1974), H is hardness in GPa, P is applied load in N and C
235 is crack radius in μm.

236 ***Shell structure.*** Scanning electron microscopy (SEM) imaging was conducted on the exterior and
237 interior of the shells collected after 16 weeks of exposure. Imaging of the exterior was done on
238 shells that had not been exposed to NaOCl (to avoid destruction of the periostracum), whereas
239 imaging of the interior surface was conducted on NaOCl-treated shells. Right shell valves were
240 affixed to an SEM stub using a copper tape and conductive paint, and sputter-coated with
241 gold/palladium. Imaging was conducted in the secondary electron imaging mode using a field
242 emission SEM (Jeol, JSM-6330F; Peabody, MA) at 3 kV and at 7-8.2 mm working distance.
243 Micrographs of the shell exteriors were taken at x 35 and x 2,500 magnifications (for the whole
244 shell and the peripheral growth ridge, respectively), and interior images were taken within a
245 central region of the shell interior at x 1,500 to x 15,000 magnifications. Six shells (three each for
246 the interior and exterior surfaces) were imaged for each treatment group.

Shell mineralogy. The right valves of clam shells collected after 21 weeks of experimental exposures and treated with NaOCl were ground with a mortar and pestle, pressed into a KBr pellet, and analyzed in transmittance mode on a Fourier Transform Infrared (FTIR) spectrometer (Bruker Optics, Vertex 70 FTIR, Billerica, MA). Spectra were acquired at 4 wave number resolution, 32 scans for two shells per experimental group. The 600 - 2000 cm^{-1} region of the spectra were isolated, baseline-corrected, and normalized, and the ν2, ν3 and ν4 peak positions and heights were measured using Spectrum 5.1 software (Perkin-Elmer, Santa Clara, CA). Relative crystallinity was determined based on ν2:ν3 and ν2:ν4 ratios (Beniash *et al.*, 1997; Gueta *et al.*, 2007).

Standard metabolic rate (SMR). SMR was determined as the resting oxygen consumption rate (MO_2) in juvenile clams after 2, 8, 11 and 21 weeks of experimental exposures. MO_2 was measured using Clarke-type oxygen electrodes (Qubit Systems Inc., Kingston, ON) in a water jacketed respiratory chamber (OX1LP-4ml, Qubit Systems, Kingston, ON) at 20°C in ASW at the same P_{CO2} and salinity as used in experimental exposures. Two-point calibration with air-saturated seawater and saturated Na_2SO_3 solution was conducted prior to each measurement at the respective salinity and P_{CO2}. The respirometry chamber was equipped with an adjustable air-tight plunger that allowed maintenance of a constant volume of water (2 ml) regardless of the volume of the experimental animals; therefore, no correction for the volume displacement by clams was needed. To avoid interference with post-prandial metabolism and feces excretion, juveniles were fasted for 24 h prior to the start of MO_2 recordings. For each measurement, 3-5 similarly sized individuals were selected, placed in the chamber, and allowed to recover from handling stress for 45 min. The chambers were closed and MO_2 measured as a decrease in O_2 concentration for 30 min. Oxygen

levels during the measurement period were never less than 80% of air saturation. Two technical replicates, with 15 minutes recovery period between the recordings, were done for each measurement and these two measurements were averaged. After each experiment, the electrode drift was determined by measuring the oxygen consumption for 15 min in the chamber with 2 ml of seawater without the clams. These values were used to correct the oxygen consumption rates of the experimental clams. A total of 10 biological replicates were obtained for each treatment group, each replicate representing SMR of a separate group of 3-5 clams. After measurements, total tissue dry mass was determined for all juveniles in the group as described above in "Shell mass and tissue mass". SMR was calculated as follows:

$$SMR = \frac{\Delta P_{O2} \times \beta_{O2} \times V}{M_{tot}} \times \left(\frac{M_{ind}}{M_{av}} \right)^{-0.2},$$

where SMR – normalized oxygen consumption (μmol O_2 g^{-1} dry mass h^{-1}), ΔP_{O2} – a decrease in partial oxygen pressure in the respirometry chamber over time (kPa h^{-1}), V – water volume in the chamber (l), β_{O2} – oxygen capacity of water (μmol O_2 l^{-1} kPa^{-1}), M_{tot} - total dry tissue mass of all juveniles in the respirometry chamber (g), M_{ind} – average individual dry tissue mass of juveniles in the respirometry chamber (mg), M_{av} – average individual dry tissue mass of juveniles across all experimental treatments (0.237 mg) and -0.2 – allometric coefficient (Lannig *et al.*, 2006).

Statistical analysis. Experimental data sets were tested for the presence of potential outliers using Grubbs' test (extreme studentized deviate method) as implemented in GraphPad Prizm ver. 5.03 (GraphPad Software, Inc., La Jolla, CA, USA). A small number of statistically significant outliers was detected and removed from the analysis; the outlier occurrence was random among the treatment groups. Regression analyses were performed to determine the relationship between

shell or tissue mass and aragonite saturation level. Linear, exponential and quadratic curves were fit to the data, and the best fit curves chosen based on the significance of the fit and the percent of variation explained by the regression line estimated by R^2. Average monthly mortalities were estimated from the weekly mortality counts in different treatment groups and compared among treatments using Fisher's exact test. The effects of the factors "P_{CO2}" and "Salinity", and their interactions on shell mechanical properties and SMR were tested using a generalized linear model (GLM) ANOVA after testing for the normality of data distribution and homogeneity of variances. Both factors were treated as fixed, and P_{CO2} had three levels (~395, 800 and 1500 µatm) while salinity had two levels (32 and 16). Post-hoc tests (Fisher's Least Significant Difference) were used to test the differences between the group means; only planned contrasts were used. Pearson correlation (R) and principal component analyses (PCA) were conducted using Origin 8.6 software (OriginLab, Northhampton, MA). Pearson correlation analysis for individual shell mass (M_{sh}) vs. tissue mass (M_{ti}) were conducted for each experimental group at 16 and 21 week time points. Furthermore, Pearson correlation and PCA analyses were conducted across all experimental groups and time points; for this analysis we used average values of SMR, $M_{sh,}$ $M_{ti,}$ and mortality for each treatment group at the respective time point with exposure time, salinity, $P_{CO2,}$ and the degree of aragonite saturation (Ω_{arg}) as the potential explanatory variables.

Sample sizes for all experimental groups were 360-505 for mortality estimates and 6-40 for all other traits. Each replicate represents a sample from an individual clam, except SMR where each biological replicate represents a group of 3-5 juveniles. Unless otherwise indicated, data are represented as means ± standard errors of means (S.E.M.). The differences were considered significant if the probability of Type I error was less than 0.05.

RESULTS

Seawater chemistry. Aragonite saturation state decreased with increasing P_{CO2} and with decreasing salinity (Table 1). An increase in P_{CO2} from ~395 to ~1500 µatm resulted in a reduction in Ω_{Arg} from Ω=4.83 to 1.46, and a similar decrease of Ω_{Arg} (to 1.54) was seen when salinity was reduced from 32 to 16 under the current P_{CO2} conditions (~395 µatm). At the low salinity (16), two experimental P_{CO2} treatments (~800 and 1500 µatm) resulted in undersaturation of the seawater for aragonite (Ω_{Arg} =0.77-0.42). In all other experimental treatments, Ω_{Arg} values were above the saturation threshold for aragonite (Table 1).

Mortality. Juvenile clams exhibited significantly higher mortality in low salinities (Fisher Exact Test: $P<0.05$ for 8-20 weeks of exposure) (Fig. 1A). In the high salinity groups P_{CO2} had no effect on mortality of juvenile clams during the first 12 weeks of exposure. After 16 weeks of exposure at salinity 32, mortality of juveniles was significantly lower at ~800 µatm P_{CO2} (<2%) than at ~1500 µatm P_{CO2} (~3-7%) or ~395 µatm (13-26%) ($P<0.05$ among all P_{CO2} groups). Mortality was also lower in clams exposed for 20 weeks to ~1500 µatm P_{CO2} at salinity 32 compared to their normocapnic counterparts ($P<0.05$); no mortality data are available for this time point for clams kept at ~800 µatm P_{CO2}. At salinity 16, the highest mortality was observed in juveniles exposed to extreme hypercapnia (~1500 µatm P_{CO2}) after 8-20 weeks of exposure ($P<0.05$ for contrasts between extreme hypercapnia and the other two P_{CO2} treatments) (Fig. 1A). Mortality of juveniles exposed to moderate hypercapnia (~800 µatm P_{CO2}) and salinity 16 was slightly but significantly lower than in the normocapnic low salinity group after 8-12 weeks of exposure ($P<0.05$) but not after prolonged (16-20 weeks) exposure ($P>0.05$).

Standard metabolic rate (SMR). SMR of clams was significantly affected by the interaction of P_{CO2} and salinity indicating that metabolic response to P_{CO2} was modulated by the acclimation salinity (Table 2). At high salinity, P_{CO2} had no significant effect on SMR (Fig. 1B). At all P_{CO2} levels, there was a slight but significant increase in SMR after 8 weeks of exposure, which quickly returned back to the initial levels in all high salinity treatments. In contrast, in low salinity groups, there was an initial depression of SMR after 2 weeks of exposure followed by a dramatic increase (by 8- to 10-fold) after 8-11 weeks of exposure (Fig. 1B). SMR peaked at different exposure times in juveniles exposed to different P_{CO2}; the maximum SMR was reached earlier in hypercapnic groups (after 8 weeks of exposure) than in the normocapnic group (after 11 weeks). After 21 weeks at low salinity, SMR has decreased in all P_{CO2} treatment groups but remained significantly elevated above the initial levels measured after 2 weeks of low salinity exposures (Fig. 1B).

Shell and tissue mass. In clams exposed to moderately elevated P_{CO2} (800 µatm) at high salinity, the shell masses (M_{sh}) were significantly higher than in the control after 16 and 21 weeks of exposure, while no difference was observed between the control (395 µatm) and extreme P_{CO2} (1500 µatm) groups maintained at high salinity (Fig. 2). At low salinity, M_{sh} values were significantly lower in all P_{CO2} treatment groups compared to their high salinity counterparts. Soft tissue mass (M_{ti}) determined after 16 weeks of exposure was also significantly lower in clams exposed to low salinity compared to their high salinity counterparts (Fig. 2). In high salinity treatments, clams exposed to hypercapnia tended to have higher tissue mass compared to their normocapnic counterparts, but this trend was only significant after 21 weeks of exposure (Fig. 2B). At low salinity, the trend was reversed, and hypercapnic groups tended to have lower tissue mass compared to their normocapnic counterparts; this trend was likewise significant only after

21 weeks of exposure (Fig. 2B). Analysis of the effects of Ω_{Arg} on shell and soft tissue mass after 16 and 21 weeks of exposure revealed a non-linear biphasic relationship between Ω_{Arg} and M_{ti} or M_{sh} (Fig. 2; $P < 0.001$, R^2=0.16-0.42 for all regressions). Shell and tissue mass were the highest at Ω_{Arg} = 3.3, which corresponds to the group exposed to moderate hypercapnia (~800 µatm P_{CO2}) at high salinity. Shell and tissue masses were reduced above and below this Ω_{Arg} and were the lowest at Ω_{Arg} <1 (Fig. 2). To better understand the relationships between M_{ti} and M_{sh} we have conducted Pearson correlation tests within each experimental treatment group. Overall, in high salinity groups the correlations between M_{ti} and M_{sh} were much stronger and highly significant compared with the low salinity treatments (Supplementary Table 1). The only exception was the control group (normocapnia at salinity 32) where no correlation between M_{ti} and M_{sh} was found after 21 weeks of exposure (Supplementary Table 1). This may be due to the fact that this group experienced high accidental mortality between 16 and 21 weeks of exposure, and the lack of correlation might be related to the survivor effect.

Mechanical properties and mineralogy of the shells. Vickers microhardness tested on the shells of clams exposed to different P_{CO2} and salinity conditions for 21 weeks, was significantly affected by P_{CO2} but not by salinity (Table 2; Fig. 3). At high salinity, shell microhardness was significantly reduced in clams exposed to ~800 and ~1500 µatm P_{CO2}. At low salinity, only the group exposed to ~1500 µatm was significantly different with respect to the shell microhardess from the respective normocapnic counterparts. Microhardness did not differ between high and low salinity treatments when groups exposed to the same P_{CO2} levels were compared ($P>0.05$).

Fracture toughness was significantly affected by the interaction of P_{CO2} and salinity indicating that the effects of elevated P_{CO2} on this trait are modulated by the exposure salinity (Table 2). At high

salinity, fracture toughness of the shells was significantly reduced in clams exposed to ~1500 µatm P_{CO2} (Fig. 3). The fracture toughness of the shells of clams exposed to ~800 µatm P_{CO2} at high salinity did not differ from the normocapnic controls despite a significantly lower hardness in the former group (Fig. 3). Shell fracture toughness was generally lower in the clams maintained at low salinity in normocapnia and moderate hypercapnia (~395 and ~800 µatm P_{CO2}) compared to their counterparts from the high salinity treatments, although the decrease was only significant at ~800 µatm P_{CO2} (Fig. 3). Interestingly, the fracture toughness values were higher in 1500 µatm $P_{CO2,}$ 16 salinity group than in 800 µatm P_{CO2}, 16 salinity group. We attribute this increase to higher porosity due to shell dissolution. The cracks generated by the indenter tip can be arrested or deflected by pores, although this porosity might or might not add to the materials strength, depending on other factors (Shigegaki *et al.*, 1997; Xu *et al.*, 2001).

FTIR spectra collected from the shells of clams exposed to different P_{CO2} and salinity regimes for 21 weeks showed that shells were comprised of aragonite with no other mineral forms present (Supplemental Figure 1). Analysis of ν_2 and ν_4 peak position and absorption intensity relative to the ν_4 peak revealed no differences among treatment groups indicating that no changes in crystallinity had occurred in response to experimental treatments (data not shown).

Shell structure. SEM imaging of the exterior (Fig. 4) and interior (Fig. 5) of the shells of clams exposed to different P_{CO2} and salinity conditions revealed distinct differences in shell structure among treatment groups. In high salinity exposures where Ω_{Arg} remained above the saturation level, only minor differences in the structure of shell exterior were observed (Fig. 4 A,B,C). Pronounced growth ridges were found in clam shells from high salinity treatments regardless of the exposure P_{CO2} (Fig. 4 A,B,C inset). At low salinity, distinct flaking of periostracum was observed

399 at all levels of P_{CO2}, with a nearly complete loss of periostracum at ~1500 µatm P_{CO2} (Fig. 4 D,E,F).
400 Major erosion and pitting of the underlying mineral were also observed at low salinity in shells of
401 the clams exposed to ~800 and 1500 µatm P_{CO2} where Ω_{Arg} was <1. Growth ridges were less
402 pronounced in the shells of clams maintained at low salinity, and at ~1500 µatm P_{CO2} and salinity
403 16 they were barely visible (Fig. 4 D,E,F inset). These results demonstrate that the exposed
404 regions of the shells are susceptible to chemical erosion in undersaturated environments.

405 In contrast, changes in structure of the interior of the shells did not vary directly with
406 experimental Ω_{Arg} levels. Under the control conditions (salinity 32, ~395 µatm P_{CO2}), the interior of
407 clam shells was composed of closely interlocking aragonite crystals (Fig. 5 A). In all other
408 experimental treatments, a distinct etching of aragonite was observed resulting in a porous
409 interior (Fig. 5). This etching was the most extreme in shells of the clams exposed to ~1500 µatm
410 P_{CO2} at low salinity (Fig. 5F). Clams exposed to ~1500 µatm P_{CO2} at low salinity also showed
411 substantial degradation and etching of the hinge region, which was not observed for other
412 treatment groups (Fig. 6).

413 ***Correlation analysis.*** Correlation analysis revealed a number of significant associations between
414 the studied parameters ($P<0.05$). As expected, Ω_{arg} of the seawater was strongly correlated with
415 salinity ($R=0.73$) and P_{CO2} ($R=-0.59$) (Supplementary Table 2). Shell mass (M_{sh}) and soft tissue
416 mass (M_{ti}) were significantly positively correlated with salinity ($R=0.64$ and 0.50, respectively)
417 and with each other ($R=0.62$). Shell mass was also positively correlated with Ω_{arg} ($R=0.39$).
418 Mortality had a strong positive correlation with exposure time ($R=0.67$) and a negative correlation
419 with salinity ($R=-0.51$), M_{ti} ($R=-0.61$) and M_{sh} (-0.39). These data indicate that changes in water

chemistry had a direct effect on tissue and shell growth as well as mortality in clams with salinity having the most profound effect.

We have tested for the possible associations between the studied parameters separately within high and low salinity groups. In the high salinity group, the only significant correlation was found between M_{ti} and M_{sh} (R=0.69) (Supplementary Table 3). In contrast, in the low salinity group a strong negative correlation was observed between P_{CO2} and M_{sh} (R=-0.55) and an equally strong positive correlation was observed between Ω_{arg} and M_{sh} (0.54), while no significant correlations were found between the water chemistry parameters and M_{ti} (Supplementary Table 4). Interestingly, exposure time was negatively correlated with M_{ti} (-0.54) indicating selective mortality and/or tissue loss in juvenile clams during prolonged exposure at low salinity.

Principal component analysis (PCA). PCA revealed that salinity and Ω_{arg} had the highest loadings on the 1st principal component (PC1) responsible for 38% of data variance (Supplementary Table 5). PC2 accounting for another 25% of variance was dominated by P_{CO2} and pH, while PC3 (15% of the variance) was predominantly associated with the experimental exposure time. Notably, PC4 accounting for 10% of the variance was dominated by SMR (a loading of 0.92); all other loadings in PC4 were very low except M_{ti} (a loading of 0.31). Together, the first three principal components (PC1, PC2 and PC3) accounted for almost 80% of the data variance. On the PCA plots, mortality and SMR grouped together in the plane formed by PC1 and PC2, consistent with the concomitant increase of SMR and mortality with decreasing salinity. There was also a strong positive relationship between salinity and shell and tissue masses. Interestingly, analysis of PC2 reveals that M_{ti} and M_{sh} are positively influenced by P_{CO2}, probably reflecting the fact that at moderately elevated P_{CO2} conditions, M_{ti} and M_{sh} values are generally higher than in normocapnia.

To eliminate possible artifacts due to the fact that pH and Ω_{arg} strongly depend on salinity and $P_{CO2,}$ we conducted PCA using only salinity, P_{CO2} and time of exposure as potential explanatory variables (Supplementary Table 6). In PC1, which accounts for 42% of variance, salinity was the dominant factor (loading 0.45). All studied biological variables had high loadings on the PC1, indicating that salinity was the major factor affecting clam biology. The exposure time dominated PC2 (a loading of 0.76) and primarily affected mortality and shell mass (Supplementary Table 6). In contrast, P_{CO2} had the highest loading (0.96) on PC3 that accounted for 15% of the variance and was weakly associated with the tissue mass and SMR (loadings of 0.18 and 0.21, respectively). An overview of the putative relationships between the experimental factors and studied biological traits based on the results of correlation and principal component analyses is shown in Figure 7.

DISCUSSION

Combined exposure to elevated P_{CO2} and reduced salinity strongly affected growth, bioenergetics and biomineralization of juvenile hard shell clams. Under the conditions of this study, salinity exerted a dominant influence on growth and bioenergetics of hard shell clams and significantly modified how shell structural and mechanical properties responded to elevated P_{CO2}. In contrast, the direct effects of P_{CO2} on biomineralization and physiology of *M. mercenaria* were small in comparison to those of salinity. This may reflect high tolerance of hard shell clams to P_{CO2} variations in the range tested in this study, but may also partially reflect the non-linear effects of P_{CO2} on some studied biological traits.

462 Acclimation of juvenile clams to low salinity resulted in a strong increase of SMR during the mid-
463 term experimental exposures (8-11 weeks) indicating elevated basal maintenance cost in these
464 organisms. During this period, SMR of clams from the low salinity group were ~3 times higher
465 than in their high salinity counterparts and ~8-10 times higher than during the initial exposure to
466 low salinity. Notably, low salinity exposure also led to an increase in activity of carbonic
467 anhydrase in gills possibly reflecting elevated need for gas exchange due to the higher SMR.
468 Elevated costs of the basal maintenance typically result in reduced aerobic scope for fitness-
469 related functions including growth (Sokolova *et al.*, 2011; Sokolova *et al.*, 2012) and a negative
470 relationship between SMR and growth rate is commonly found in marine bivalves (Hawkins *et al.*,
471 1986; Awkins and Day, 1996; Bayne and Hawkins, 1997; Fraser and Rogers, 2007).

472 High energy cost of basal maintenance also goes hand-in-hand with elevated mortality and
473 reduced shell and tissue mass in clams exposed to low salinity, indicating that energy deficiency
474 may contribute to the reduced growth and survival of this group. A similar increase in mortality
475 associated with the depletion of energy stores has been observed in juvenile oysters during the
476 combined exposure to low salinity and high CO_2 levels (Dickinson *et al.*, 2012). In the present
477 study, SMR was slightly reduced after 21 weeks of exposure at low salinity conditions (even
478 though it still remained significantly above the control levels and above SMR recorded during the
479 initial period of low salinity exposure). This moderate reduction in SMR after the long-term
480 exposure to low salinity may reflect physiological acclimation; however, if true, this would
481 indicate an unusually slow acclimation process in juvenile hard shell clams. Typically,
482 physiological acclimation to salinity shifts is completed and a new metabolic steady-state is
483 achieved within 3 to 6 weeks in marine mollusks (Berger, 1986; Prosser, 1991; Berger and

484 Kharazova, 1997). Alternatively, a decrease in SMR after 21 weeks in low salinity may be due to
485 the selective mortality of experimental clams, since the individuals with highest SMR are expected
486 to develop the strongest energy deficiency and therefore will be most prone to salinity-induced
487 stress. Indeed, earlier studies in marine bivalves showed that individuals with lower SMR are
488 more resistant to environmental stress and have higher survivorship under the stress conditions
489 (Hawkins *et al.*, 1986; Myrand *et al.*, 2002).

490 The shell mass of clams was affected by P_{CO2} and Ω_{Arg} in a non-linear manner. At moderately
491 elevated P_{CO2} (~800 µatm, salinity 32) we observed an increase in shell mass of clams compared
492 to the normocapnic counterparts. However, the average shell mass of clams exposed to extreme
493 P_{CO2} (~1500 µatm, salinity 32) was similar to those maintained in normocapnia. These
494 observations indicate that moderate acidification can increase rates of shell deposition in this
495 species, while further increase in P_{CO2} abolishes this effect. This "bell-shaped" response is even
496 more apparent when the mass data is plotted against aragonite saturation levels corresponding to
497 each experimental condition. The exact physiological mechanisms of this apparent increase in
498 shell deposition rates under the moderately hypercapnic conditions are currently not known.
499 However, a similar bell-shaped response of calcification rates to increasing P_{CO2} and decreasing in
500 Ω_{Arg} has been previously reported for other species of marine calcifiers (Doney *et al.*, 2009; Ries *et*
501 *al.*, 2009). Interestingly, many other species, including eastern oysters (*Crassostrea virginica*)
502 demonstrate a very different biomineralization response to changes of P_{CO2}, with a linear decrease
503 of shell deposition rates with increasing CO_2 levels (Ries *et al.*, 2009; Beniash *et al.*, 2010). This is
504 especially noteworthy in light of the fact that the shells of eastern oysters are made of calcite,
505 which is a more thermodynamically stable $CaCO_3$ isoform, with a higher degree of saturation than

that of aragonite under any given set of conditions. Hence, these differences in response of clams and oysters to elevated P_{CO2} indicate that biological factors may play a more significant role in the shell deposition of these species than physicochemical properties of seawater, and that biological mechanisms of biomineralization are different in these bivalve species.

Environmental P_{CO2} and salinity conditions also had profound effects on shell structure and mechanical properties of juvenile clams. Exposure to conditions where aragonite saturation was below 1 (i.e. elevated P_{CO2} and low salinity) caused significant etching of the shells' exterior surfaces. In all experimental groups in which Ω_{Arg} was above 1 the etching of the exterior was relatively modest, suggesting that erosion of the shell exterior is primarily affected by hydrochemistry. This chemical dissolution of the shells may have also contributed to the observed decrease in the shell mass of clams from the low salinity treatments compared to their counterparts maintained at high salinity. Indeed, experiments by Nenhuis and colleagues (Nienhuis *et al.*, 2010) demonstrated that a decrease in the rate of shell growth in *Nucella lamellosa* under elevated CO_2 conditions is primarily caused by higher rates of shell dissolution and not a decrease in the shell deposition rates. In the case of *M. mercenaria*, these relationships appeared more complex, since a moderate increase in the CO_2 levels led to an increase in the shell deposition rate. However, it is likely that at low Ω_{Arg} levels dissolution plays a major role in the mass balance of the shells. Shell erosion may become a major factor affecting survival of bivalves in brackish coastal and estuarine waters by weakening the shells and making them more vulnerable to predators (Green *et al.*, 2009; Amaral *et al.*, 2012).

Interestingly, etching of the shell interior was observed in all groups with elevated P_{CO2} even under the supersaturation conditions for aragonite. These observations indicate that etching of

528 the shells' interior is not directly related to the water chemistry. One possible explanation is that
529 the mollusks dissolve the interior of the shells to compensate for the effects of CO_2-induced
530 acidosis in the tissues as described in mollusks (Crenshaw, 1972; Sokolova *et al.*, 2000). SEM
531 analysis of the shells has also revealed that at low Ω_{Arg} values, a significant erosion of the material
532 in the hinge area occurred, leading to weakening of the ligament insertion site and separation of
533 the shell valves. This, in turn, can lead to a major impediment of the shell opening mechanism and
534 affect growth and survival of the mollusks. Our observations are in agreement with earlier reports
535 of compromised hinge structures in juvenile clams maintained under low aragonite saturation
536 conditions (Talmage and Gobler, 2010).

537 Salinity and Ω_{Arg} had much less effect on microhardness of the shells than $P_{CO2.}$ For example, the
538 shell microhardness of the clams exposed to normocapnia at low salinity was not significantly
539 different from the high salinity normocapnic controls although there was a 3-fold difference in
540 Ω_{Arg} between these two experimental conditions. At the same time, microhardness of the shells of
541 clams exposed to elevated CO_2 levels were significantly lower than in those from normocapnic
542 treatments. Notably, fracture toughness of the shells of clams exposed to ~800 µatm P_{CO2} at high
543 salinity did not differ from the normocapnic controls (salinity 32, ~395 µatm P_{CO2}) despite having
544 significantly lower hardness. The fracture toughness in the shells from ~1500 µatm, low salinity
545 group also did not differ significantly from the control, likely reflecting the effect of increased shell
546 porosity in limiting crack propagation (Shigegaki *et al.*, 1997; Xu *et al.*, 2001). Taken together,
547 these data indicate that factors other than chemical erosion contributed to the differences in shell
548 hardness and fracture toughness in clams exposed to different salinity and P_{CO2} levels. It is
549 possible that elevated CO_2 may affect the structural organization of the shell mineral and organic

components and/or the proportion of the organic matrix to the mineral in the shell, which in turn will affect its mechanical properties. Determination of the precise biological and structural mechanisms underlying these effects of elevated P_{CO2} is outside the scope of this study and requires further investigation.

As a corollary, our study demonstrates complex interactive effects of salinity and P_{CO2} on physiology and biomineralization of hard shell clams. The major effects of low salinity under the conditions of this study are driven by the elevated basal energy demand that can lead to energy deficiency, reduced growth and elevated mortality of juvenile clams, and possibly to impaired shell maintenance as evidenced by the extensive damage to the periostracum at low salinity. The effects of elevated P_{CO2} on physiology and biomineralization of hard shell clams appear to be more complex and subtle. The metabolic effects of high P_{CO2} in the studied range (~380-1500 µatm) are minimal, while the most pronounced changes are seen with respect to the growth and mechanical properties of the shell. Effects of elevated P_{CO2} on biomineralization of hard shell clams involve a complex interplay between the chemical effects of corrosive seawater and biological responses to elevated P_{CO2} and/or reduced Ω_{Arg}. Moderate hypercapnia (~ 800 µatm P_{CO2}) appears to stimulate shell and tissue growth and reduce mortality of juvenile clams; however, exposure to low salinity or extreme hypercapnia (~ 1500 µatm P_{CO2}) abates these effects. Mechanical properties of the shell (such as microhardness and fracture toughness) are negatively affected by elevated CO_2 alone or in combination with low salinity, which may have important implications for protection against predators or environmental stressors. Overall, our data indicate that environmental salinity may strongly modulate responses to ocean acidification in hard shell clams as well as

571 other marine bivalves (Dickinson *et al.*, 2012) and thus should be taken into account when
572 predicting the effects of ocean acidification on estuarine ecosystems.

573 ACKNOWLEDGEMENTS

574 This work was supported by funds provided by NSF award IOS-0951079 to I.M.S and E.B.

575

577 Addadi L., Joester D., Nudelman F., Weiner S. (2006) Mollusk Shell Formation: A Source of New Concepts for
578 Understanding Biomineralization Processes. ***Chemistry - A European Journal*** **12**:980-987.
579 Amaral V., Cabral H.N., Bishop M.J. (2011) Resistance among wild invertebrate populations to recurrent
580 estuarine acidification. ***Estuarine Coastal and Shelf Science*** **93**:460-467.
581 Amaral V., Cabral H.N., Bishop M.J. (2012) Effects of estuarine acidification on predator-prey interactions.
582 ***Marine Ecology-Progress Series*** **445**:117-127.
583 Anstis G.R., Chantikul P., Lawn B.R., Marshall D.B. (1981) A Critical Evaluation of Indentation Techniques for
584 Measuring Fracture Toughness: I. Direct Crack Measurements. ***J. Am. Ceram. Soc.*** **64**: 533-538.
585 Awkins A.J.S., Day A.J. (1996) The metabolic basis of genetic differences in growth efficiency among marine
586 animals. ***Journal of Experimental Marine Biology and Ecology*** **203**:93-115.
587 Baldassarri M., Margolis H.C., Beniash E. (2008) Compositional Determinants of Mechanical Properties of
588 Enamel. ***Journal of Dental Research*** **87**:645-649.
589 Bayne B.L., Hawkins A.J.S. (1997) Protein metabolisms the costs of growth and genomic heterozygosity:
590 experiments with the mussel *Mytilus galloprovincialis Lmk*. ***Physiological zoology*** **710**:391-402.
591 Beniash E., Aizenberg J., Addadi L., Weiner S. (1997) Amorphous calcium carbonate transforms into calcite
592 during sea urchin larval spicule growth. ***Proceedings of the Royal Society of London Series B-***
593 ***Biological Sciences*** **264**:461-465.
594 Beniash E., Ivanina A., Lieb N.S., Kurochkin I., Sokolova I.M. (2010) Elevated levels of carbon dioxide affect
595 metabolism and shell formation in oysters *Crassostrea virginica*. ***Marine Ecology Progress Series***
596 **419**:95-108.
597 Berger V.J. (1986) ***Adaptations of marine molluscs to changes of environmental salinity*** "Nauka". 216
598 pp., Leningrad.
599 Berger V.J., Kharazova A.D. (1997) Mechanisms of salinity adaptations in marine molluscs. ***Hydrobiologia***
600 **355**:115-126.
601 Burnett L.E. (1997) The challenges of living in hypoxic and hypercapnic aquatic environments. ***American***
602 ***Zoologist*** **37**:633-640.
603 Byrne M., Ho M., Wong E., Soars N.A., Selvakumaraswamy P., Shepard-Brennand H., Dworjanyn S.A., Davis
604 A.R. (2011) Unshelled abalone and corrupted urchins: Development of marine calcifiers in a
605 changing ocean. ***Proceedings of the Royal Society B: Biological Sciences*** **278**:2376-2383.
606 Cai W.J., Wang Y. (1998) The chemistry, fluxes, and sources of carbon dioxide in the estuarine waters of the
607 Satilla and Altamaha Rivers, Georgia. ***Limnology and Oceanography*** **43**:657-668.
608 Cooley S., Doney S. (2009) Anticipating ocean acidification's economic consequences for commercial
609 fisheries. ***Environmental Research Letters*** **4**:open access.
610 Crenshaw M.A. (1972) The inorganic composition of molluscan extrapallial fluid. ***Biol Bull*** **143**:506-512.
611 Currey J.D., Taylor J.D. (1974) The mechanical behaviour of some molluscan hard tissues. ***Journal of***
612 ***Zoology*** **173**:395-406.
613 Dickinson G.H., Ivanina A.V., Matoo O.B., Pörtner H.O., Lannig G., Bock C., Beniash E., Sokolova I.M. (2012)
614 Interactive effects of salinity and elevated CO_2 levels on juvenile eastern oysters, *Crassostrea*
615 *virginica*. ***The Journal of Experimental Biology*** **215**:29-43.
616 Dickson A.G. (1990) Standard potential of the ($AgCl(s) + 1/2H_2(g) = Ag(s) + HCl(aq)$) cell and the
617 dissociation constant of bisulfate ion in synthetic sea water from 273.15 to 318.15 K. ***J. Chem.***
618 ***Thermodynamics*** **22**:113-127.
619 Doney S.C., Fabry V.J., Feely R.A., Kleypas J.A. (2009) Ocean acidification: The other CO_2 problem. ***Annual***
620 ***Review of Marine Science*** **1**:169-192.
621 Dupont S., Dorey N., Thorndyke M. (2010) What meta-analysis can tell us about vulnerability of marine
622 biodiversity to ocean acidification? ***Estuarine, Coastal and Shelf Science*** **89**:182-185.

Fraser K.P.P., Rogers A.D. (2007) Protein metabolism in marine animals: the underlying mechanisms of growth. ***Advances in Marine Biology*** **52**:267-632.
Gazeau F., Quiblier C., Jansen J.M., Gattuso J.P., Middelburg J.J., Heip C.H.R. (2007) Impact of elevated CO_2 on shellfish calcification. ***Geophysical Research Letters*** **34**.
Green M.A., Waldbusser G.G., Reilly S.L., Emerson K., O'Donnell S. (2009) Death by dissolution: Sediment saturation state as a mortality factor for juvenile bivalves. ***Limnol Oceanogr*** **54**.
Gueta R., Natan A., Addadi L., Weiner S., Refson K., Kronik L. (2007) Local atomic order and infrared spectra of biogenic calcite. ***Angewandte Chemie-International Edition*** **46**:291-294.
Gutiérrez J.L., Jones C.G., Strayer D.L., Iribarne O.O. (2003) Mollusks as ecosystem engineers: the role of shell production in aquatic habitats. ***Oikos*** **101**:79-90.
Hawkins A.J.S., Bayne B.L., Day A.J. (1986) Protein Turnover, Physiological Energetics and Heterozygosity in the Blue Mussel, *Mytilus edulis*: The Basis of Variable Age-Specific Growth. ***Proceedings of the Royal Society of London. Series B, Biological Sciences*** **229**:161-176.
Kleypas J.A., Feely R.A., Fabry V.J., Langdon C., Sabine C.L., Robbins L.L. (2006) Impacts of Ocean Acidification on Coral Reefs and Other Marine Calcifiers. A Guide for Future Research. ***Report of a workshop sponsored by NSF, NOAA and the US Geological Survey***:88pp.
Kochmann J., Buschbaum C., Volkenborn N., Reise K. (2008) Shift from native mussels to alien oysters: Differential effects of ecosystem engineers. ***Journal of Experimental Marine Biology and Ecology*** **364**:1-10.
Kraeuter J.N., Castagna M.E. (2001) ***Biology of the Hard Clam*** Elsevier Science.
Kroeker K.J., Kordas R.L., Crim R.N., Singh G.G. (2010) Meta-analysis reveals negative yet variable effects of ocean acidification on marine organisms. ***Ecology Letters*** **13**:1419-1434.
Lannig G., Eilers S., Pörtner H.O., Sokolova I.M., Bock C. (2010) Impact of ocean acidification on energy metabolism of oyster, *Crassostrea gigas*—changes in metabolic pathways and thermal response. ***Marine Drugs*** **8**:2318-2339.
Lannig G., Flores J.F., Sokolova I.M. (2006) Temperature-dependent stress response in oysters, *Crassostrea virginica*: Pollution reduces temperature tolerance in oysters. ***Aquatic Toxicology*** **79**:278-287.
Lewis E., Wallace D.W.R. (1998) Program Developed for CO_2 System Calculations. ***ORNL/CDIAC-105. Carbon Dioxide Information Analysis Center, Oak Ridge National Laboratory, U.S. Department of Energy, Oak Ridge, Tennessee***.
McElhany P., Busch S.D. (2012) Appropriate pCO_2 treatments in ocean acidification experiments. ***Marine Biology***:1-6.
Mook W.G., Koene B.K.S. (1975) Chemistry of dissolved inorganic carbon in estuarine and coastal brackish waters. ***Estuarine and Coastal Marine Science*** **3**:325-336.
Myrand B., Tremblay R., Sevigny J.-M. (2002) Selection Against Blue Mussels (Mytilus edulis L.) Homozygotes Under Various Stressful Conditions. ***J Hered*** **93**:238-248.
Najjar R.G., Pyke C.R., Adams M.B., Breitburg D., Hershner C., Kemp M., Howarth R., Mulholland M.R., Paolisso M., Secor D., Sellner K., Wardrop D., Wood R. (2010) Potential climate-change impacts on the Chesapeake Bay. ***Estuarine, Coastal and Shelf Science*** **86**:1-20.
Nienhuis S., Palmer A.R., Harley C.D.G. (2010) Elevated CO_2 affects shell dissolution rate but not calcification rate in a marine snail. ***Proceedings of the Royal Society B-Biological Sciences*** **277**:2553-2558.
Nikinmaa M. (2013) Climate change and ocean acidification—Interactions with aquatic toxicology. ***Aquatic Toxicology*** **126**:365-372.
Pörtner H. (2008a) Ecosystem effects of ocean acidification in times of ocean warming: a physiologist's view. ***Marine Ecology Progress Series*** **373**:203-217.
Pörtner H.O. (2008b) Ecosystem effects of ocean acidification in times of ocean warming: a physiologist's view. ***Marine Ecology Progress Series*** **373**:203-217.
Pörtner H.O. (2012) Integrating climate-related stressor effects on marine organisms: unifying principles linking molecule to ecosystem-level changes. ***Marine Ecology Progress Series*** **470**:273-290.

672 Prosser C.L. (1991) ***Environmental and Metabolic Animal Physiology*** Wiley-Liss, New york etc.
673 Przeslawski R., Ahyong S., Byrne M., Worheide G., Hutchings P. (2008) Beyond corals and fish: the effects of
674 climate change on noncoral benthic invertebrates of tropical reefs. ***Global Change Biology***
675 **14**:2773-2795.
676 Ries J.B., Cohen A.L., McCorkle D.C. (2009) Marine calcifiers exhibit mixed responses to CO_2-induced ocean
677 acidification. ***Geology*** **37**:1131-1134.
678 Ringwood A.H., Keppler C.J. (2002) Water quality variation and clam growth: Is pH really a non-issue in
679 estuaries. ***Estuaries*** **25**:901-907.
680 Shigegaki Y., Brito M.E., Hirao K., Toriyama M., Kanzaki S. (1997) Strain tolerant porous silicon nitride.
681 ***Journal of the American Ceramic Society*** **80**:495-498.
682 Sokolova I.M., Bock C., Pörtner H.O. (2000) Resistance to freshwater exposure in White Sea *Littorina* spp. II:
683 Acid-base regulation. ***Journal of Comparative Physiology B: Biochemical, Systemic, and***
684 ***Environmental Physiology*** **170**:105-115.
685 Sokolova I.M., Frederich M., Bagwe R., Lannig G., Sukhotin A.A. (2012) Energy homeostasis as an integrative
686 tool for assessing limits of environmental stress tolerance in aquatic invertebrates. ***Marine***
687 ***Environmental Research*** **79**:1-15.
688 Sokolova I.M., Sukhotin A.A., Lannig G. (2011) Stress effects on metabolism and energy budgets in mollusks
689 ***In: Oxidative Stress in Aquatic Ecosystems. D. Abele, T. Zenteno-Savin, J. Vazquez-Medina (eds).***
690 ***Blackwell Wiley, Boston etc.***:263-280.
691 Stanley S.M. (2006) Influence of seawater chemistry on biomineralization throughout phanerozoic time:
692 Paleontological and experimental evidence. ***Palaeogeography, Palaeoclimatology, Palaeoecology***
693 **232**:214–236.
694 Talmage S.C., Gobler C.J. (2010) Effects of past, present, and future ocean carbon dioxide concentrations on
695 the growth and survival of larval shellfish. ***Proceedings of the National Academy of Sciences of the***
696 ***United States of America*** **107**:17246-17251.
697 Thomsen J., Gutowska M.A., Saphörster J., Heinemann A., Trübenbach K., Fietzke J., Hiebenthal C.,
698 Eisenhauer A., Körtzinger A., Wahl M., Melzner F. (2010) Calcifying invertebrates succeed in a
699 naturally CO2-rich coastal habitat but are threatened by high levels of future acidification.
700 ***Biogeosciences*** **7**:3879-3891.
701 Tomanek L., Zuzow M.J., Ivanina A.V., Beniash E., Sokolova I.M. (2011) Proteomic response to elevated pCO_2
702 level in eastern oysters, *Crassostrea virginica*: evidence for oxidative stress. ***The Journal of***
703 ***Experimental Biology*** **214**:1836-1844.
704 Waldbusser G., Voigt E., Bergschneider H., Green M., Newell R. (2011) Biocalcification in the eastern oyster
705 (*Crassostrea virginica*) in relation to long-term trends in Chesapeake Bay pH. ***Estuaries and Coasts***
706 **34**:221-231.
707 Xu H.H.K., Quinn J.B., Takagi S., Chow L.C., Eichmiller F.C. (2001) Strong and macroporous calcium
708 phosphate cement: Effects of porosity and fiber reinforcement on mechanical properties. ***Journal of***
709 ***Biomedical Materials Research*** **57**:457-466.

710

711

712 FIGURE CAPTIONS

713 **Figure 1**. Mortality and standard metabolic rate (SMR) in juvenile clams exposed to different P_{CO2}
714 and salinity treatments.

715 A – mortality over 20 weeks of exposure period. Solid symbols and solid lines – salinity 32; open
716 symbols and broken lines – salinity 16. Circles, squares and triangles correspond to exposure P_{CO2}
717 of ~395, 800 and 1500 µatm, respectively. There are no mortality estimates for juveniles exposed
718 to ~800 µatm P_{CO2}, salinity 32, due to an accidental loss of experimental animals. N=360-505. B –
719 SMR measured as mass-specific oxygen consumption rates standardized to the average mass of
720 experimental clams (0.237 mg dry tissue mass). Different letters denote significant differences
721 between exposure periods within the same experimental condition ($P<0.05$). Asterisks denote the
722 values that are significantly different from the respective values for the control clams (maintained
723 at ~395 µatm P_{CO2} and salinity 32) for the same duration of time ($P<0.05$). Vertical bars represent
724 standard error. N=9-10.

725 **Figure 2.** Changes in *M. mercenaria* shell and tissue mass in response to salinity, P_{CO2} and
726 aragonite saturation. A - average shell mass after 16 and 21 weeks of exposure; B - average tissue
727 mass after 16 and 21 weeks of exposure. Different letters denote significant differences between
728 different P_{CO2} levels at the same salinity and exposure period ($P< 0.05$). * represent significant
729 differences between different high and low salinity at the same P_{CO2} levels and exposure period
730 ($p< 0.05$). C & E – regressions of shell mass vs. aragonite saturation levels after 16 and 21 weeks of
731 exposure, respectively; D & F – regressions of tissue mass vs. aragonite saturation levels after 16

and 21 weeks of exposure, respectively. Polynomial regressions (solid lines) and 95% confidence intervals (broken lines) are given. N=11-40 in each experimental group.

Figure 3. Mechanical properties of the shells of *M. mercenaria* exposed to different P_{CO2} and salinities levels.

A – Vickers microhardness of clam shells exposed to experimental conditions for 21 weeks. B – fracture toughness of clam shells exposed to experimental conditions for 21 weeks. Within each graph, groups marked with different letters are significantly different ($p < 0.05$). * represents significant difference between high and low salinity groups at same P_{CO2}. Data are presented as mean, and the vertical bars show S.E.M. N=6-7.

Figure 4. SEM micrographs of the exterior of *M. mercenaria* shells after 16 weeks exposure to experimental conditions. Inset on each panel is a high magnification image of a growth ridge near the periphery of the shell. A – 395 µatm, salinity 32; B – 395 µatm, salinity 16; C – 800 µatm, salinity 32; D – 800 µatm, salinity 16; E – 1500 µatm, salinity 32; F – 1500 µatm, salinity 16. Scale bars: 500 µm outer panel; 5 µm inset.

Figure 5. SEM micrographs of the interior of *M. mercenaria* shells after 16 weeks exposure to experimental conditions. Images were taken within the center region of the shell interior. Higher (inset) and lower (outer) magnification images were taken from the same region. A – 395 µatm, salinity 32; B – 395 µatm, salinity 16; C – 800 µatm, salinity 32; D – 800 µatm, salinity 16; E – 1500 µatm, salinity 32; F – 1500 µatm, salinity 16. Scale bars: 100 µm outer panel; 1 µm inset.

Figure 6. SEM micrographs of the interior of the hinge region of *M. mercenaria* shells after 16 weeks exposure to experimental conditions. A – 395 µatm, salinity 32; B – 1500 µatm, salinity 16.

753 **Figure 7**. A schematic representation of the relationships between the environmental factors
754 (blue ovals) and the studied biological traits (green ovals). Black and red connector lines
755 represent relationships with positive and negative correlations, respectively. Solid lines represent
756 significant correlations (based on Pearson correlation analysis). Dashed lines represent
757 relationships which did not show significant Pearson correlation coefficients but were identified
758 as important by PCA. Arrows identify putative causality and numbers by the connector lines are
759 Pearson correlation coefficients (R). Abbreviations: P_{CO2}- partial pressure of CO_2; Exp- duration of
760 experimental exposure; Ω_{arg}- aragonite saturation; Sal-salinity; M_{ti}- tissue mass; M_{sh}- shell mass;
761 SMR- standard metabolic rate; Mrt- mortality.

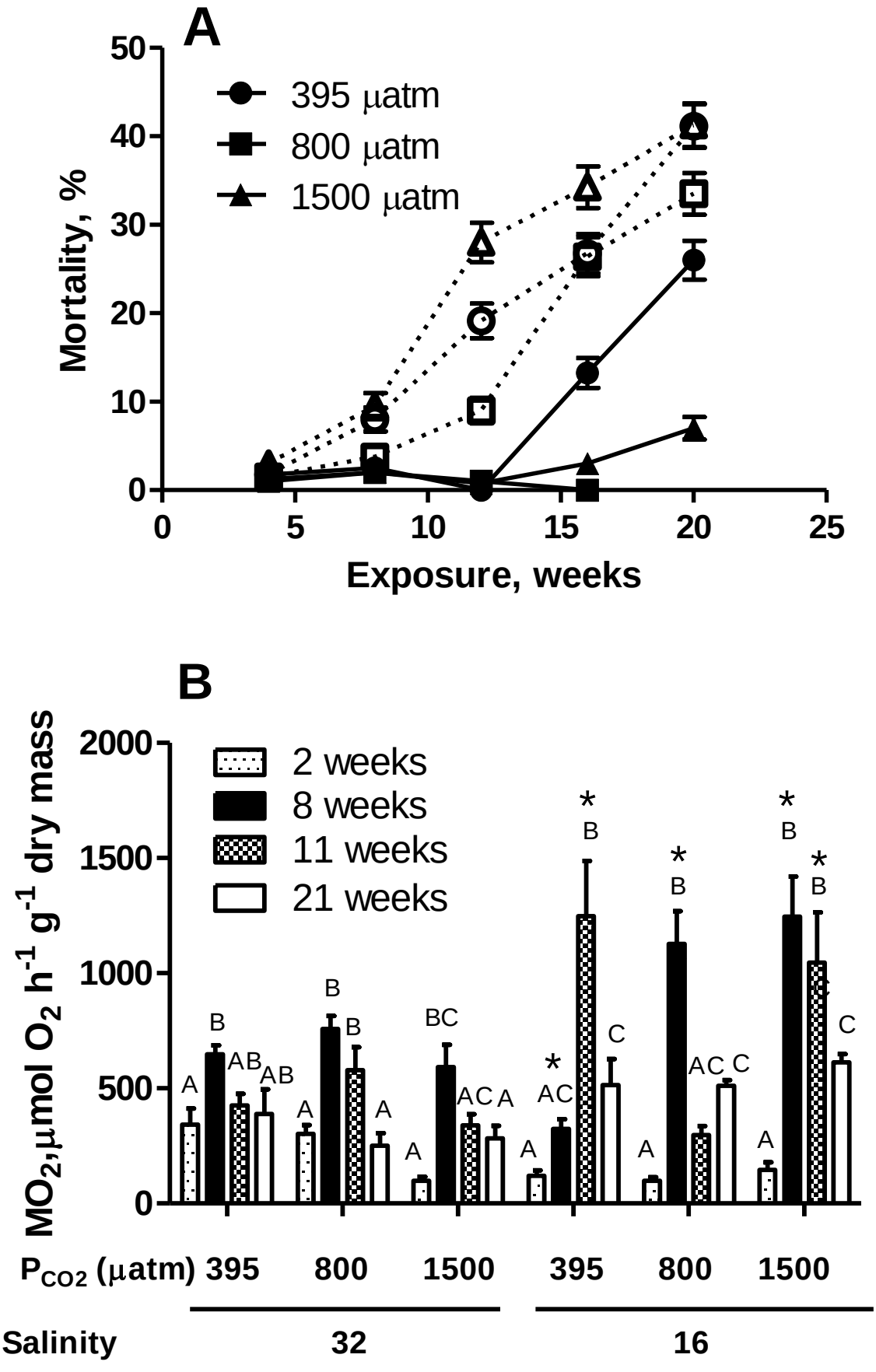

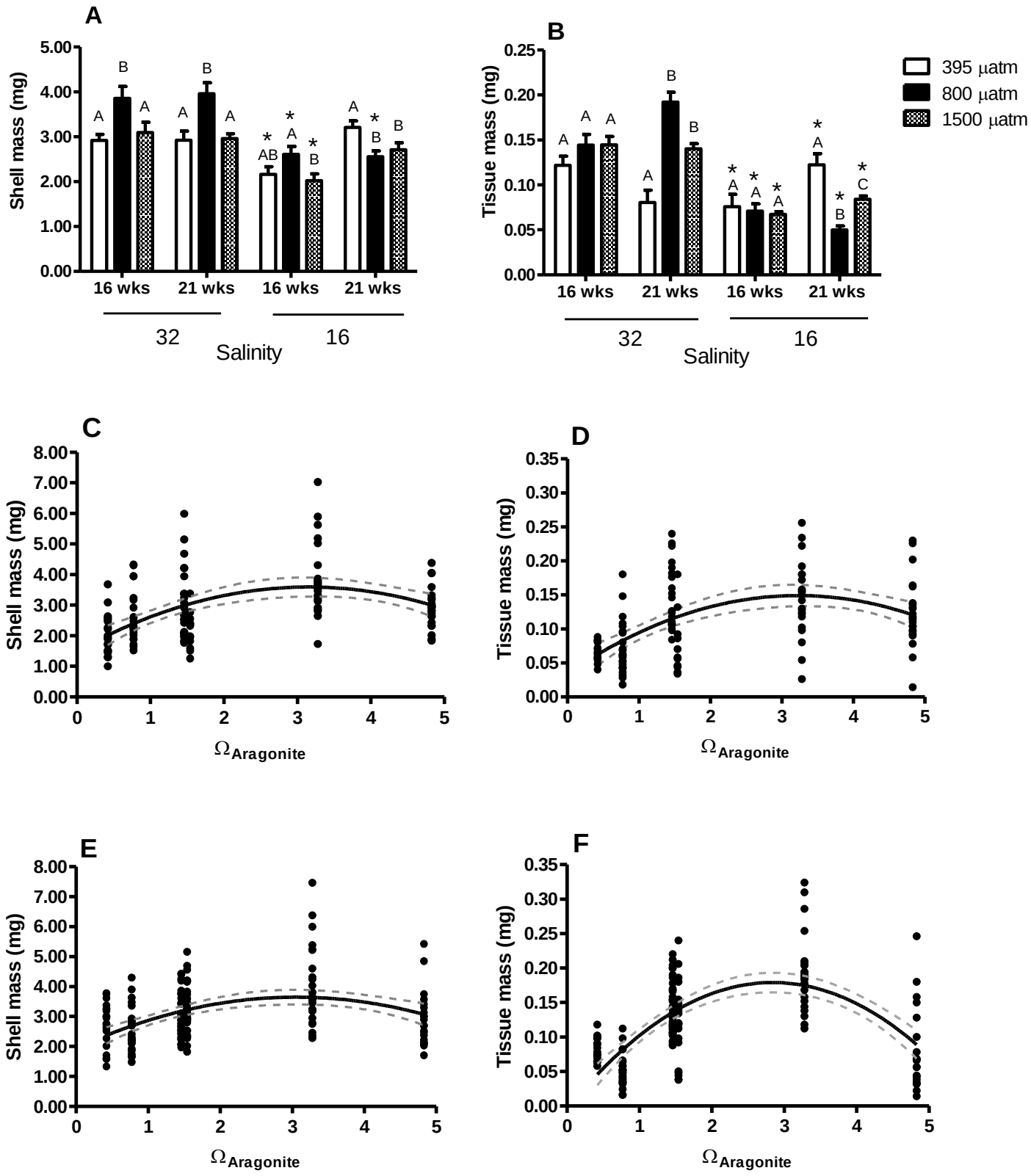

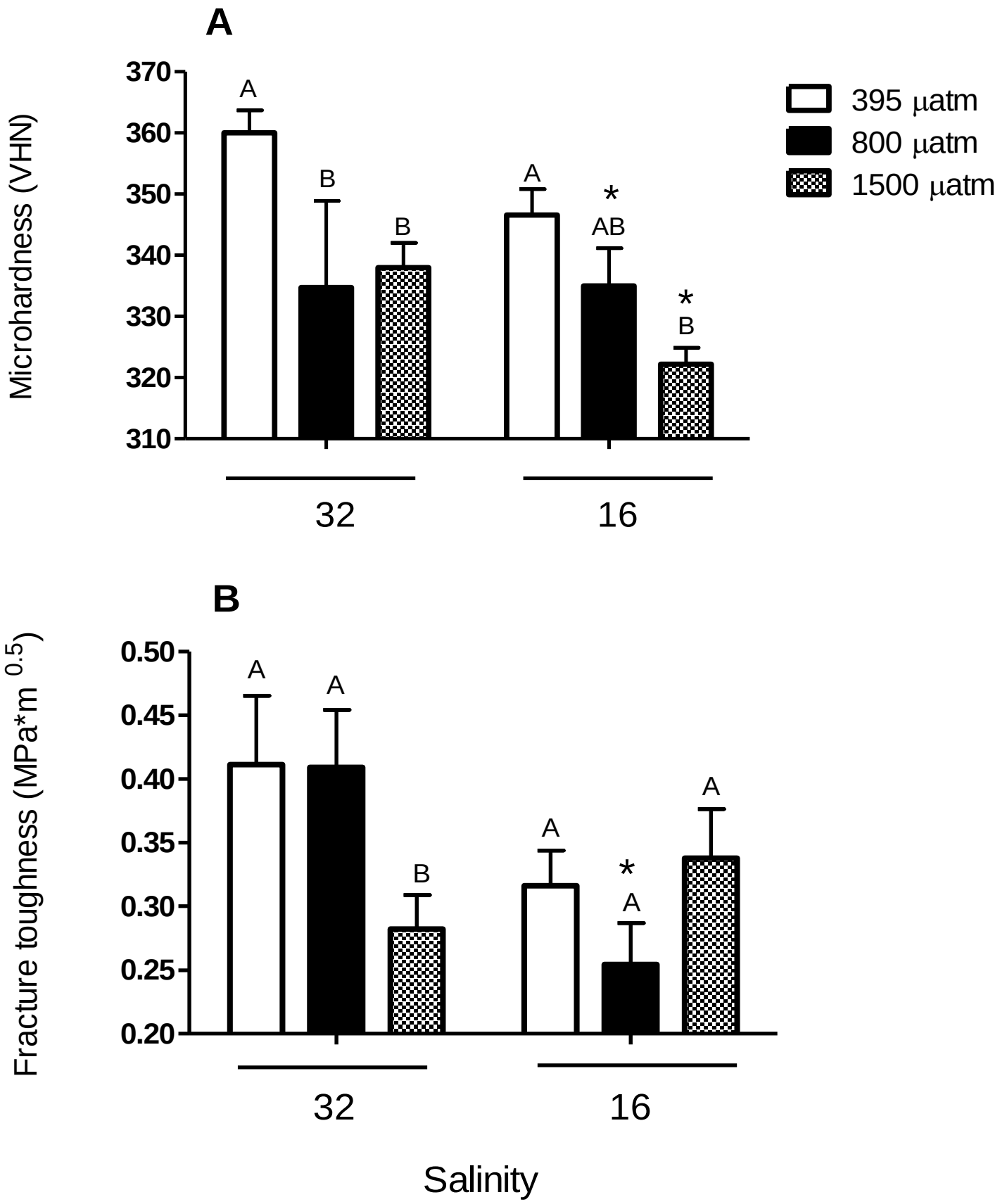

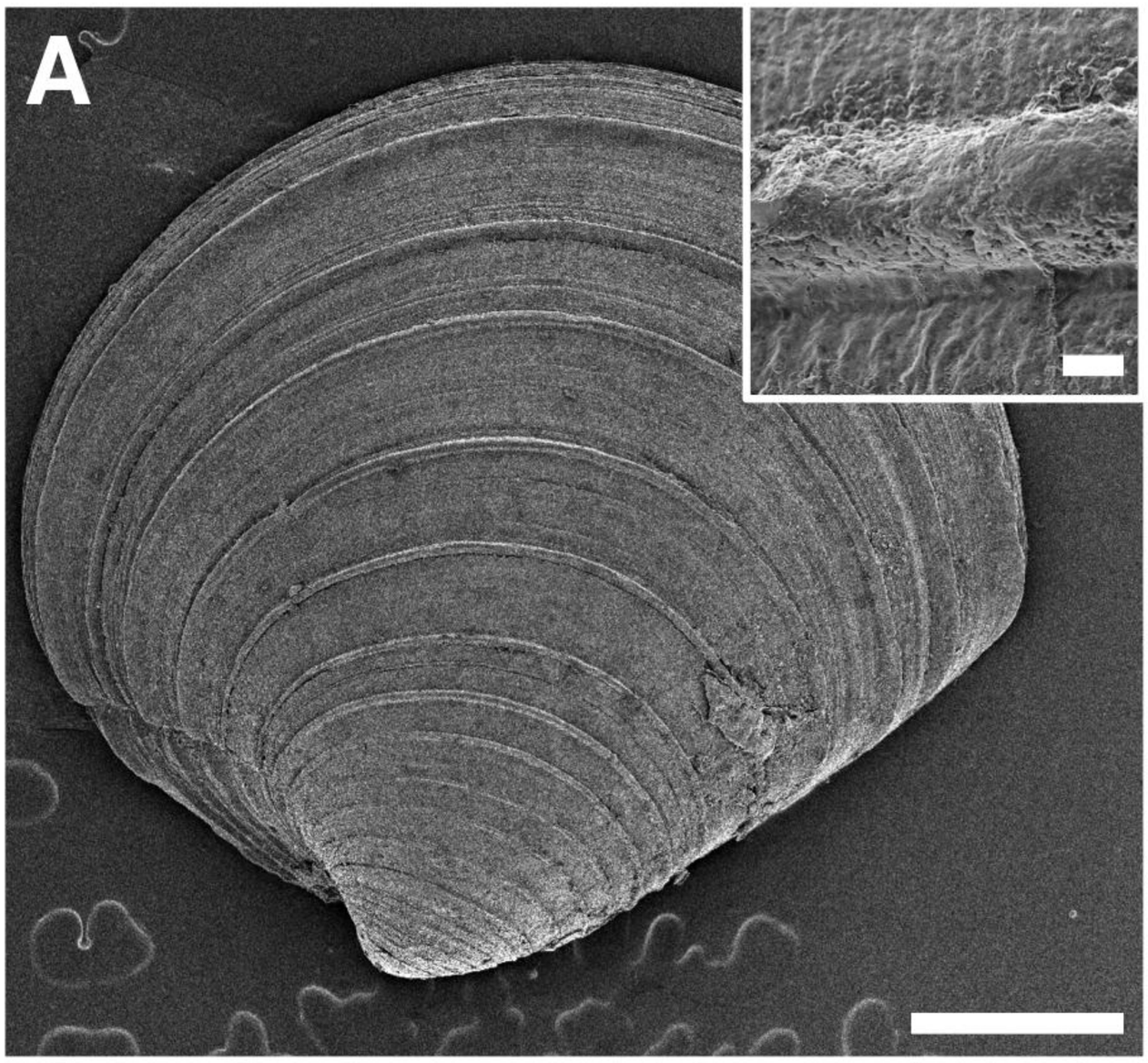
A

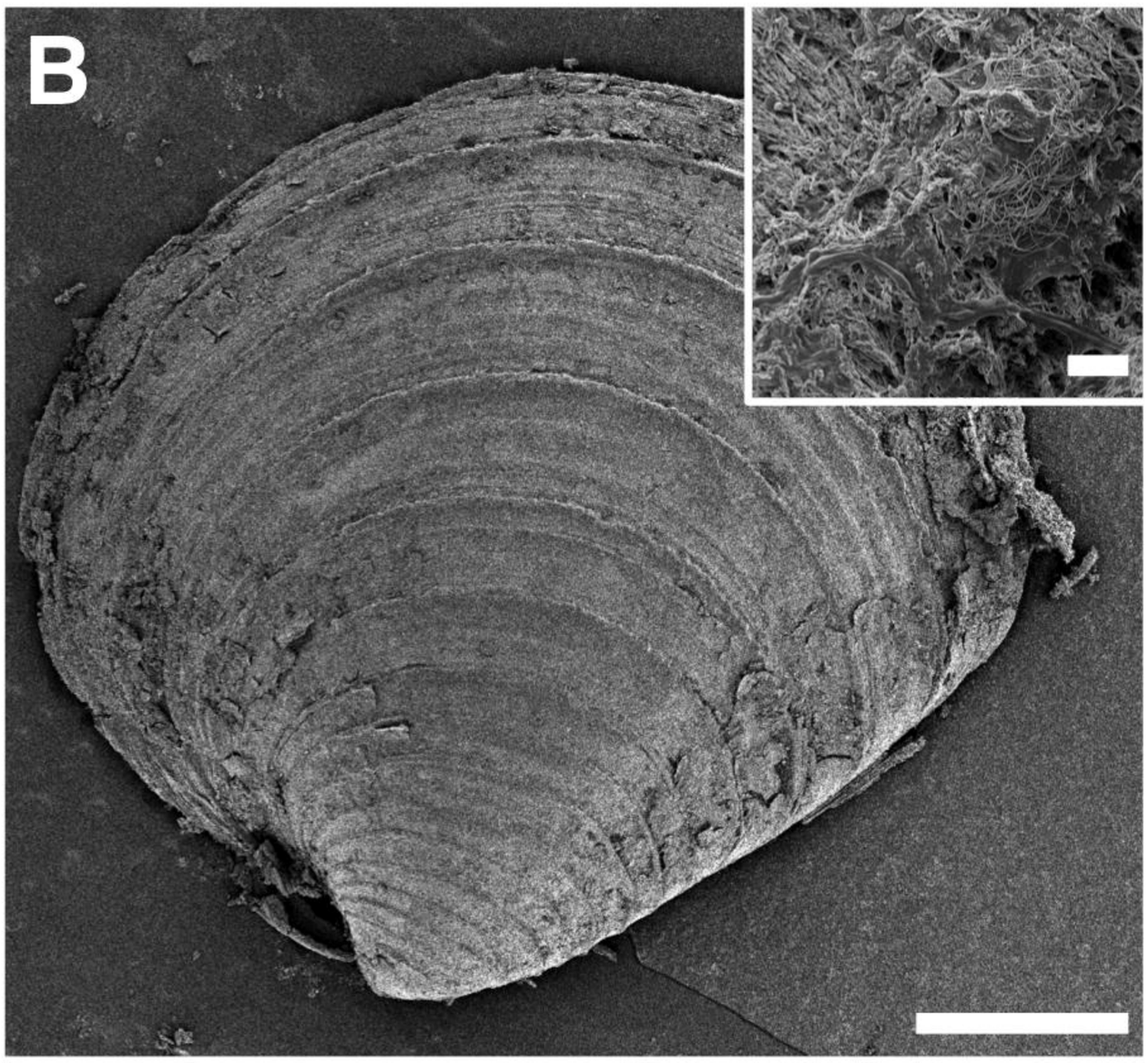
B

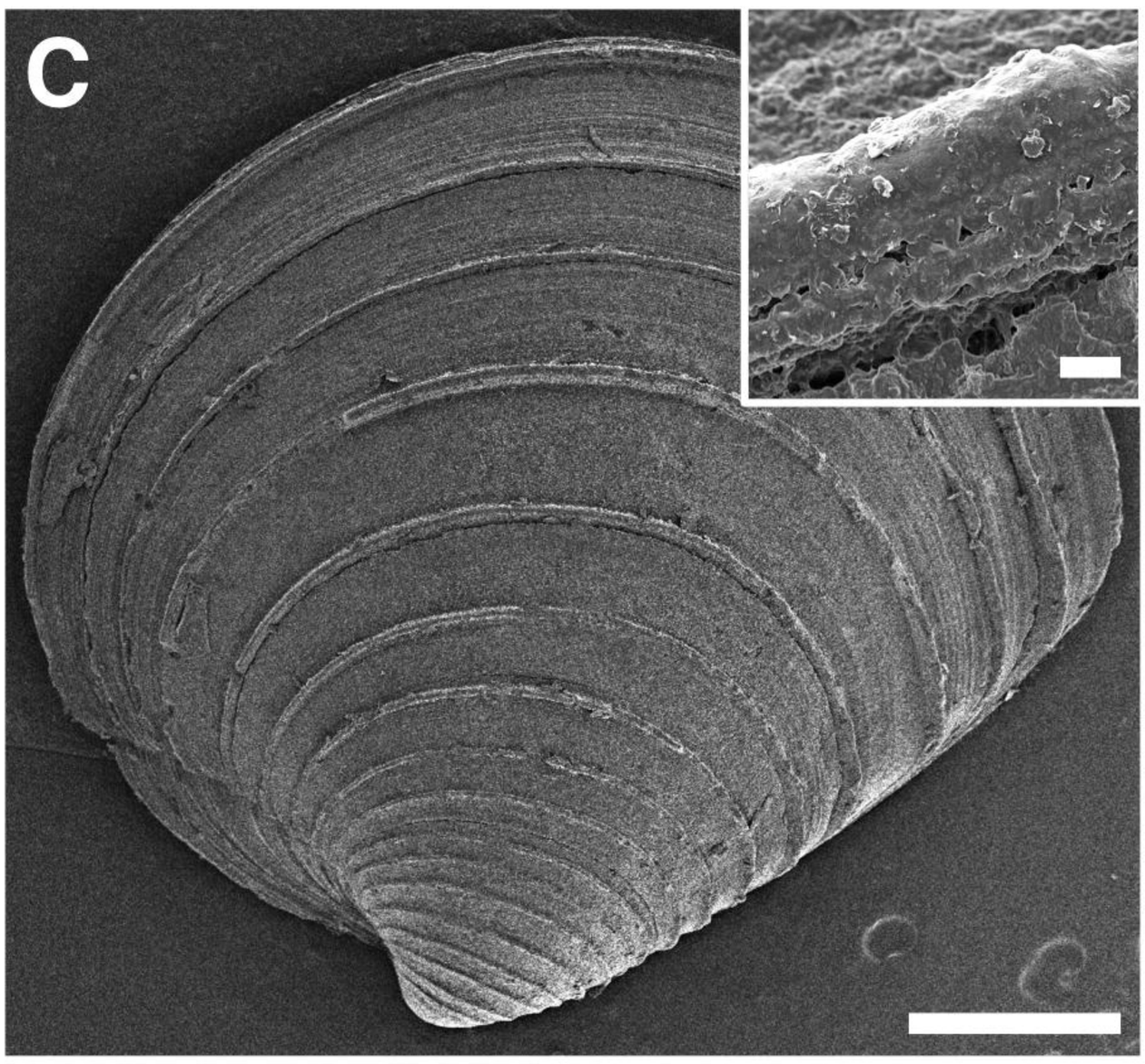
C

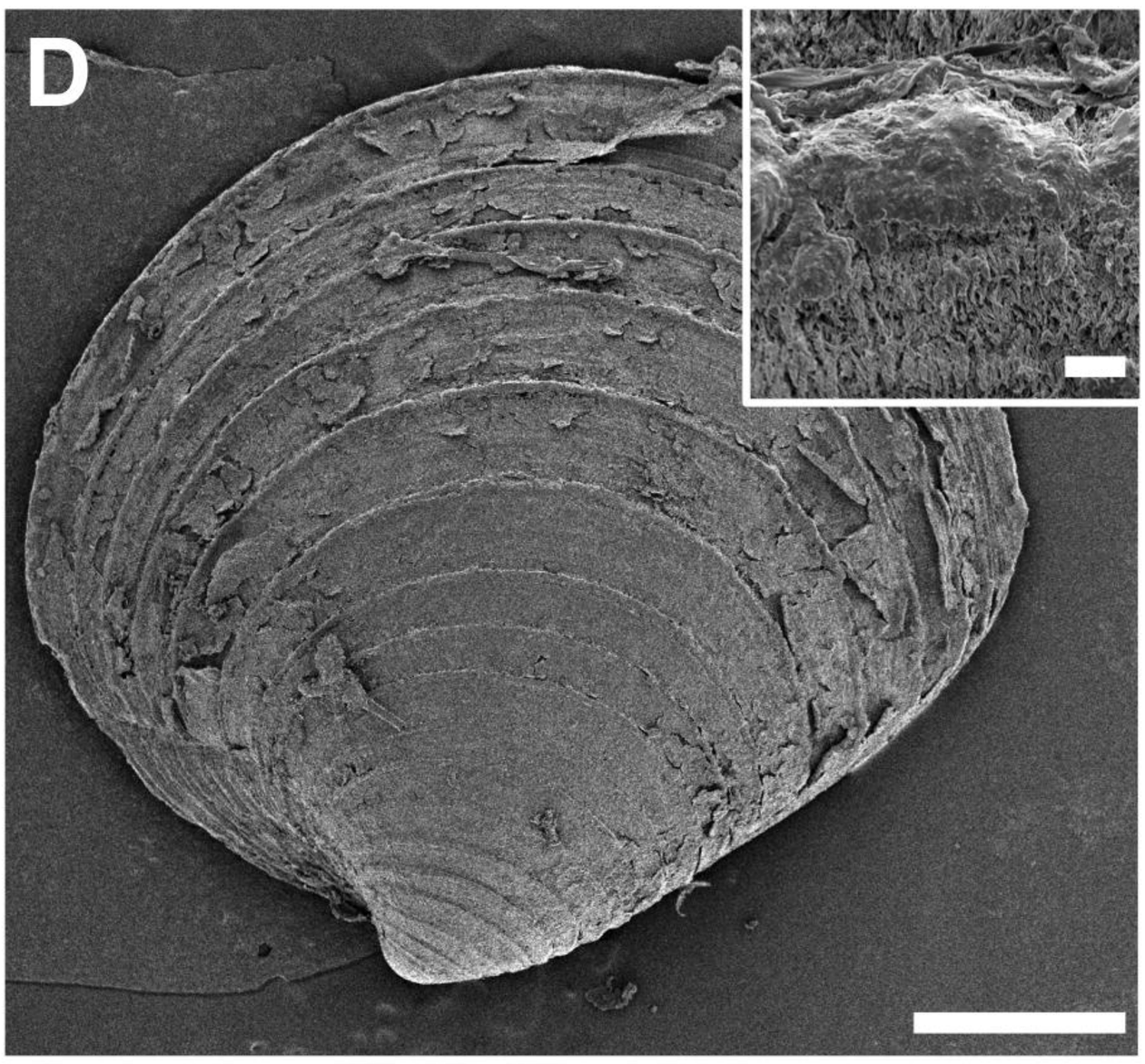
D

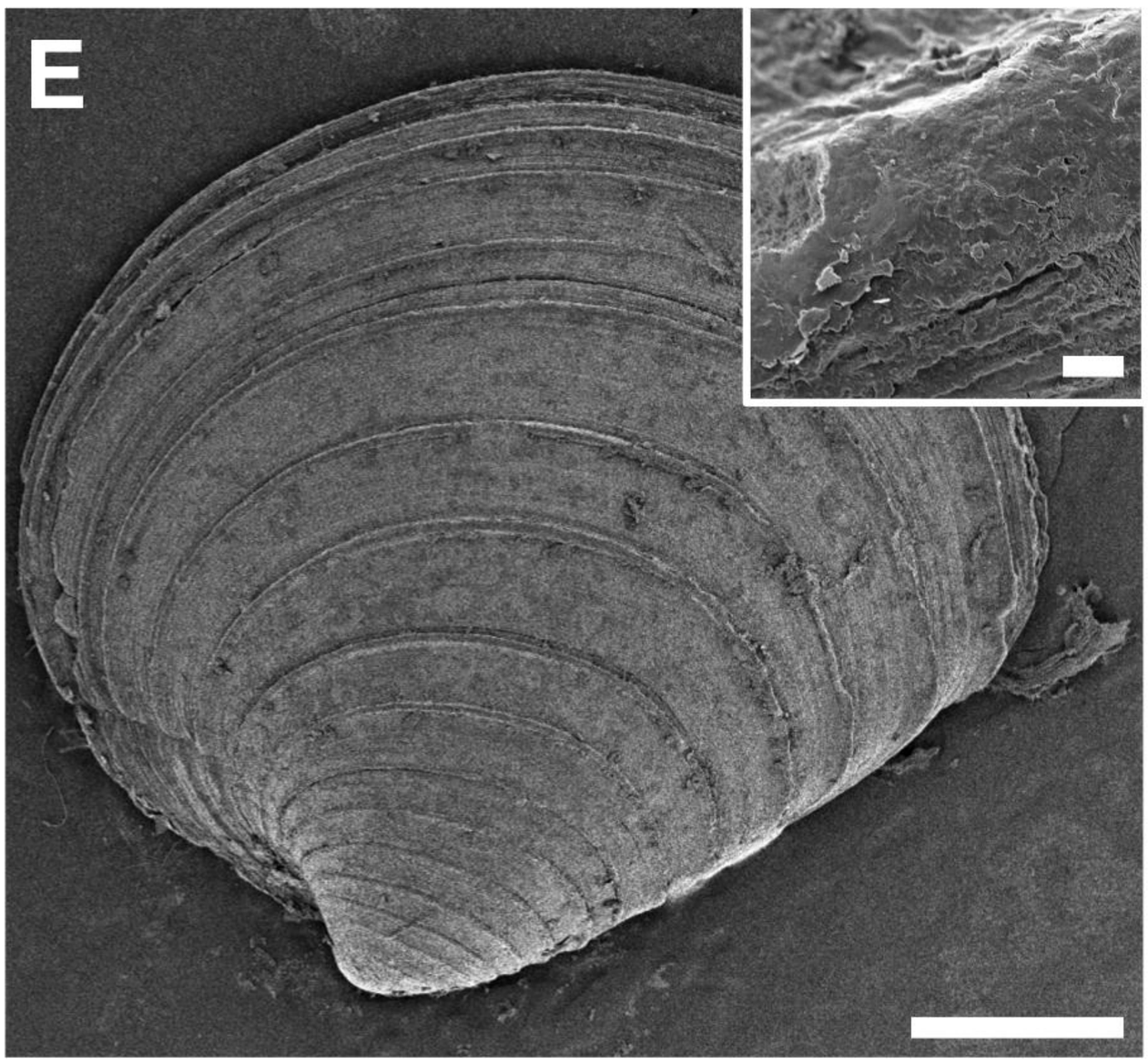
E

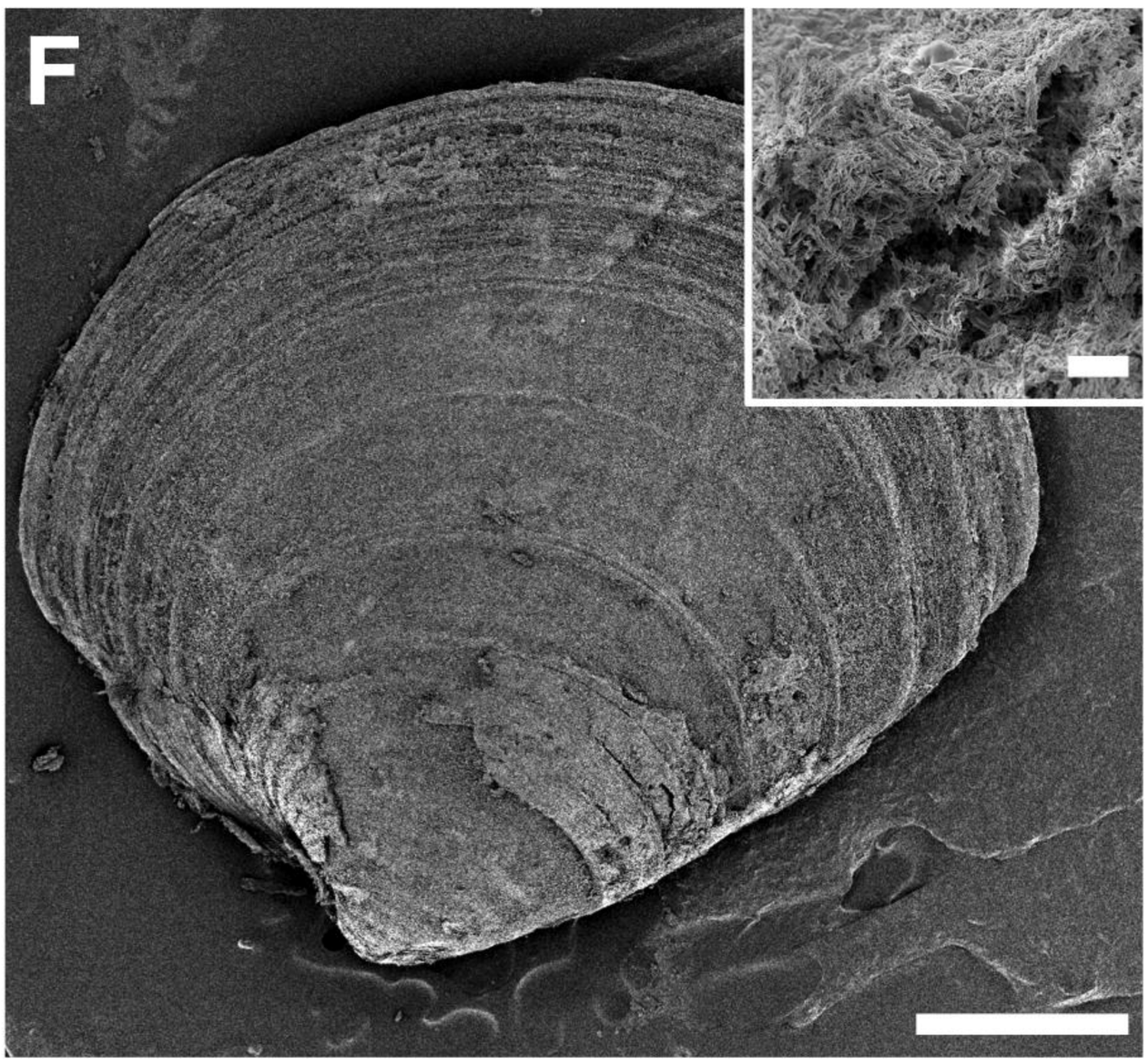
F

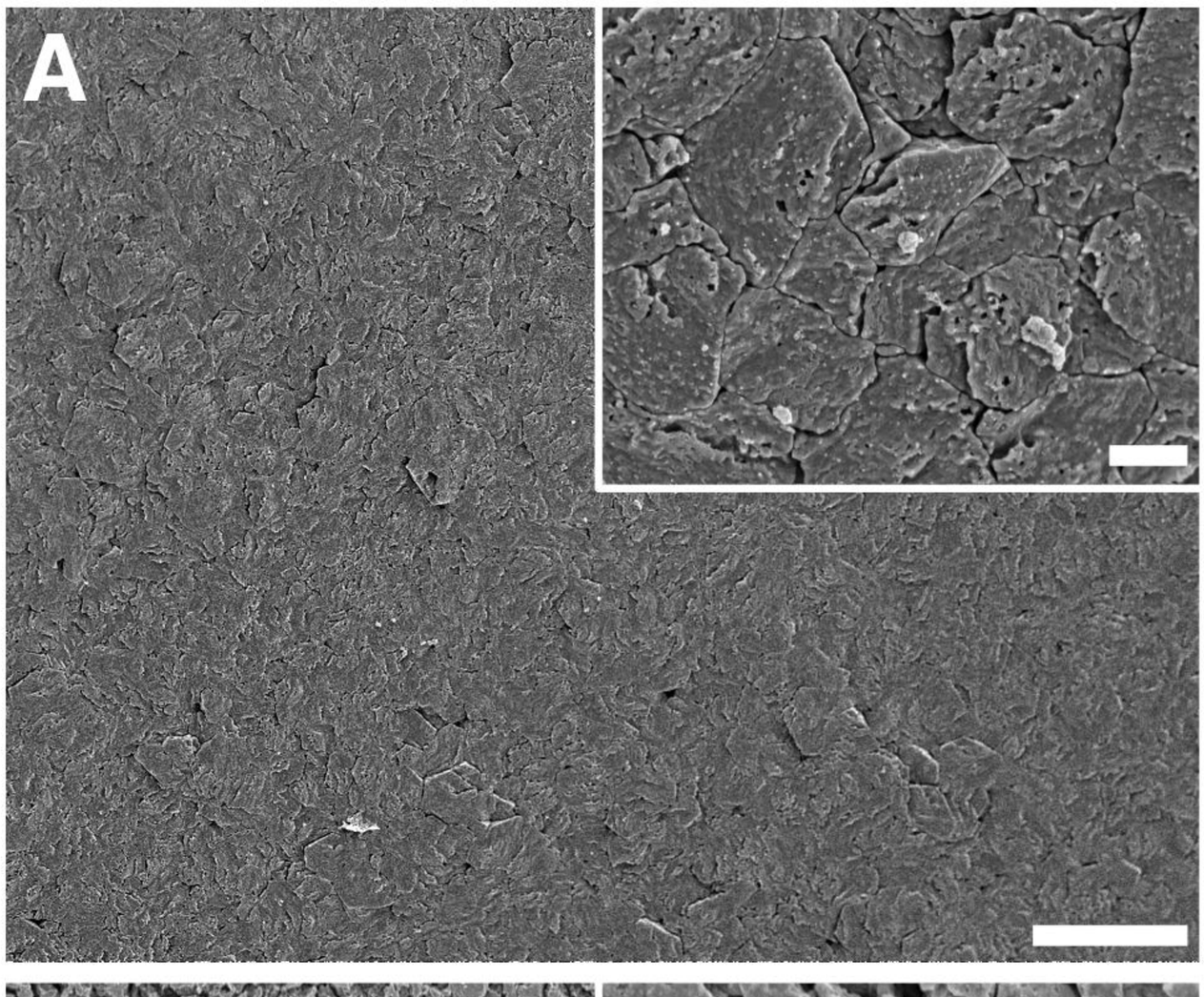
A

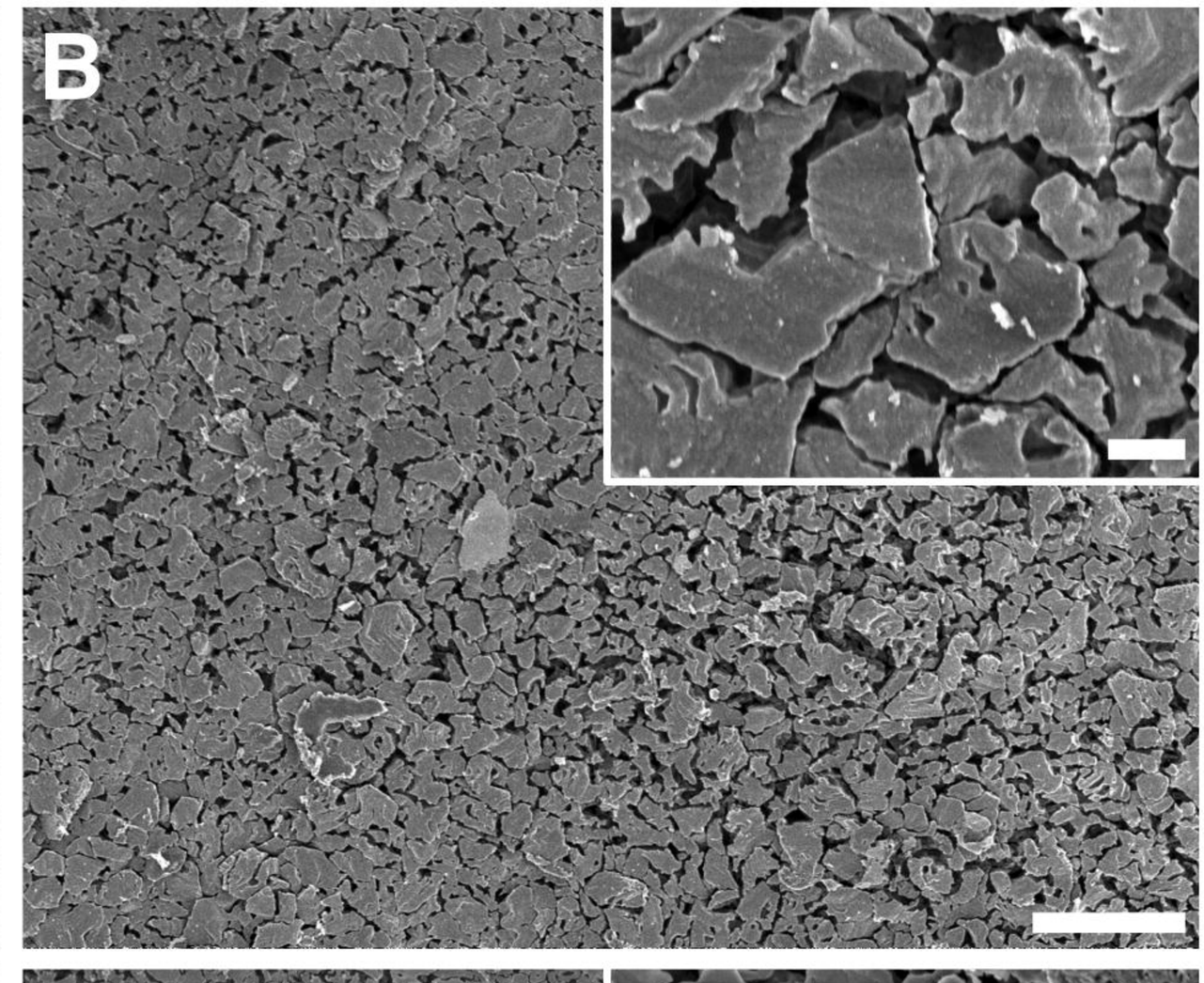
B

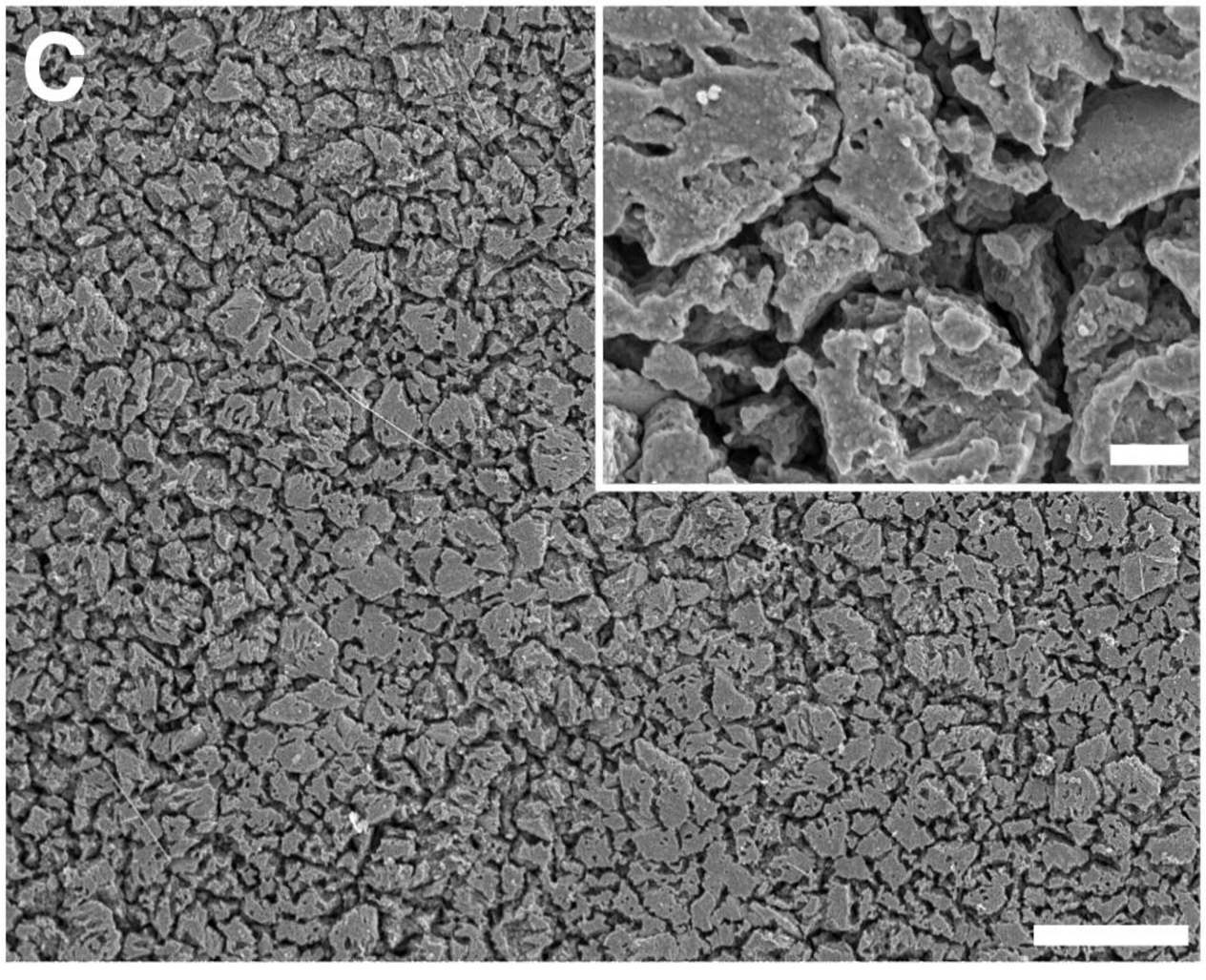
C

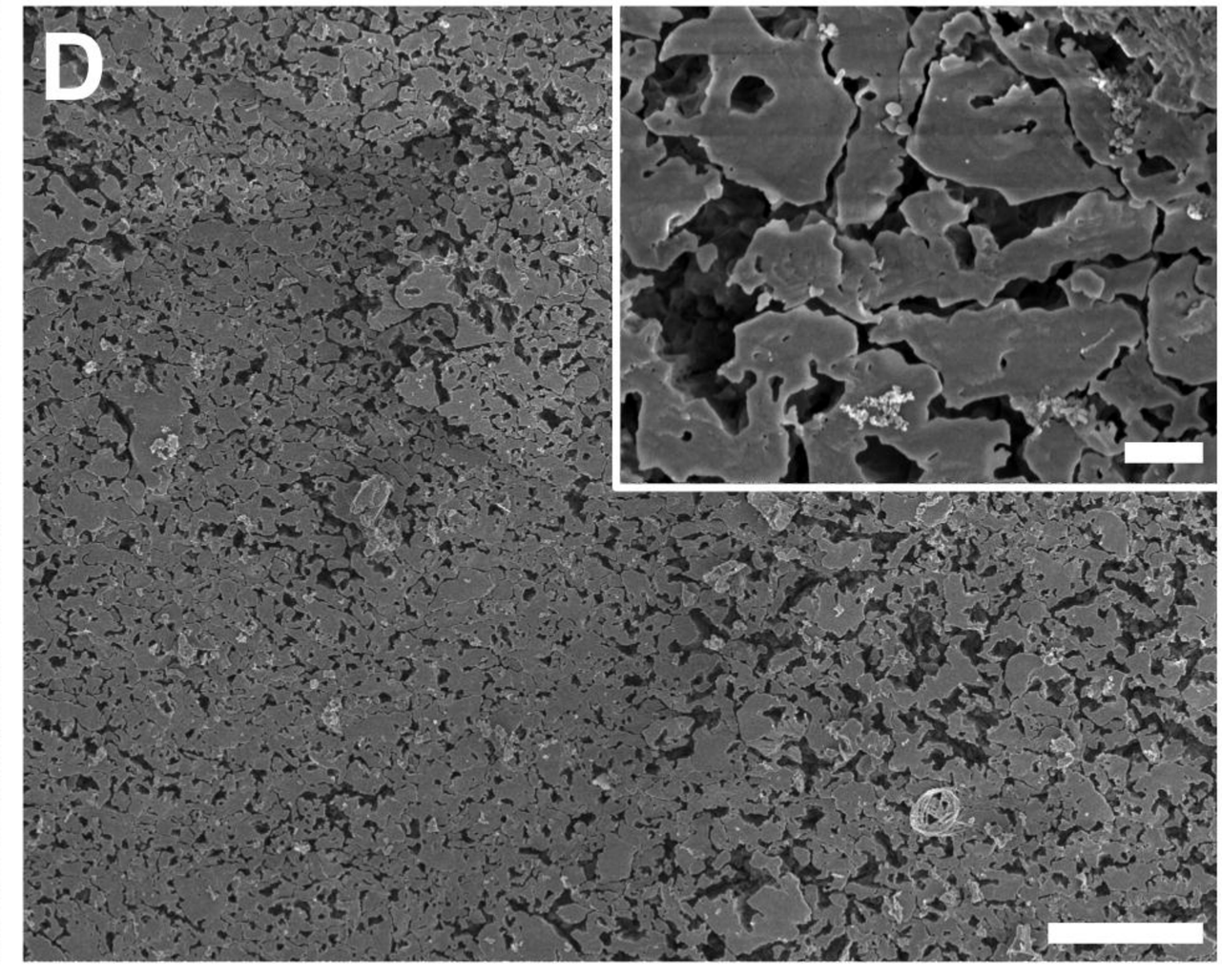
D

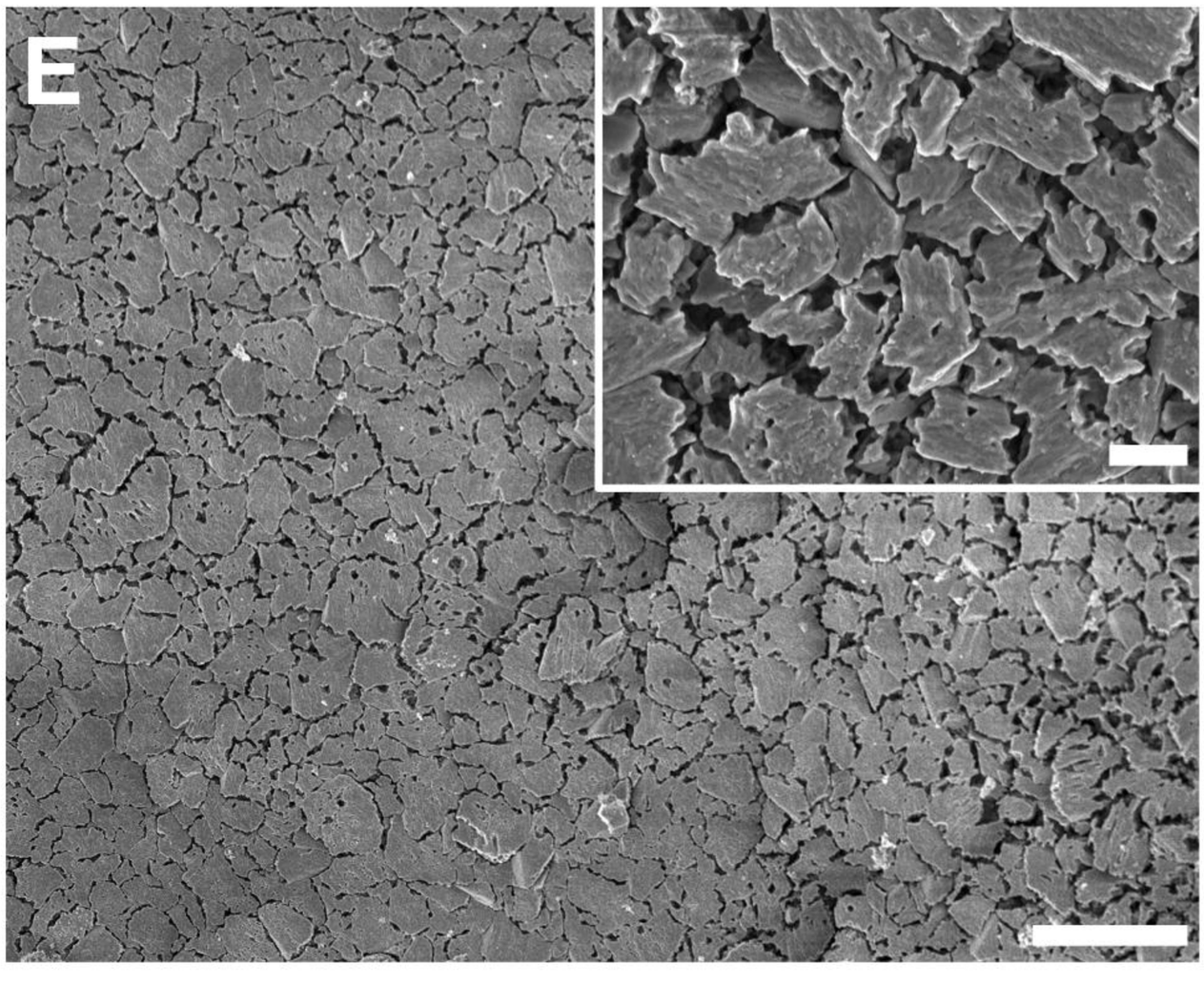
E

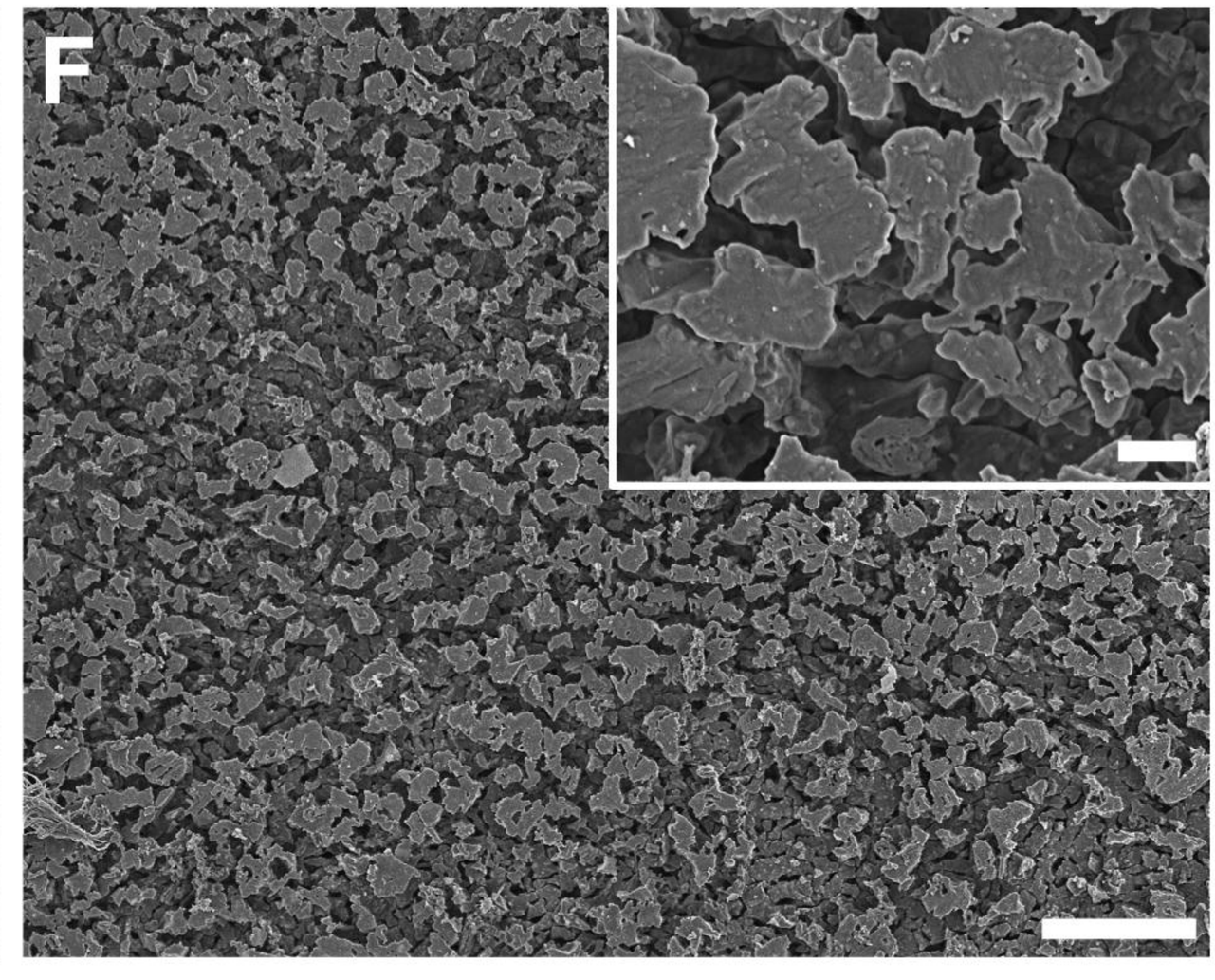
F

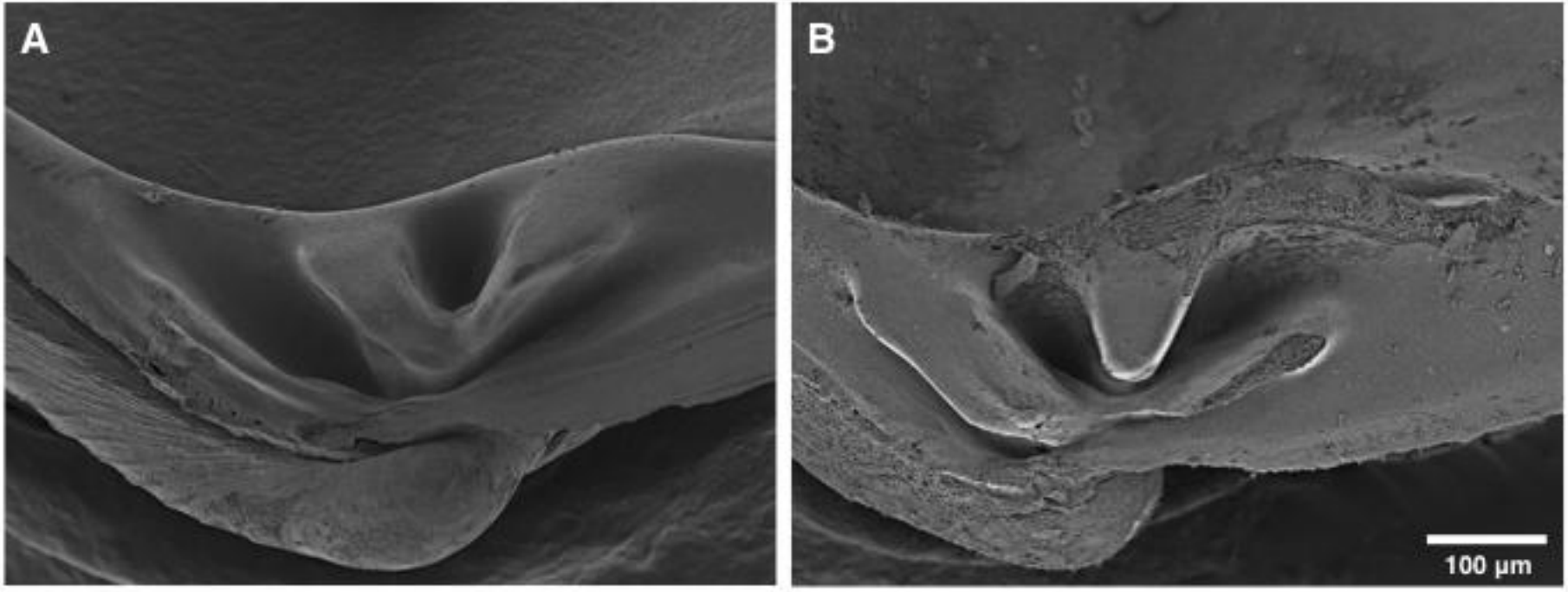
A
B
100 µm

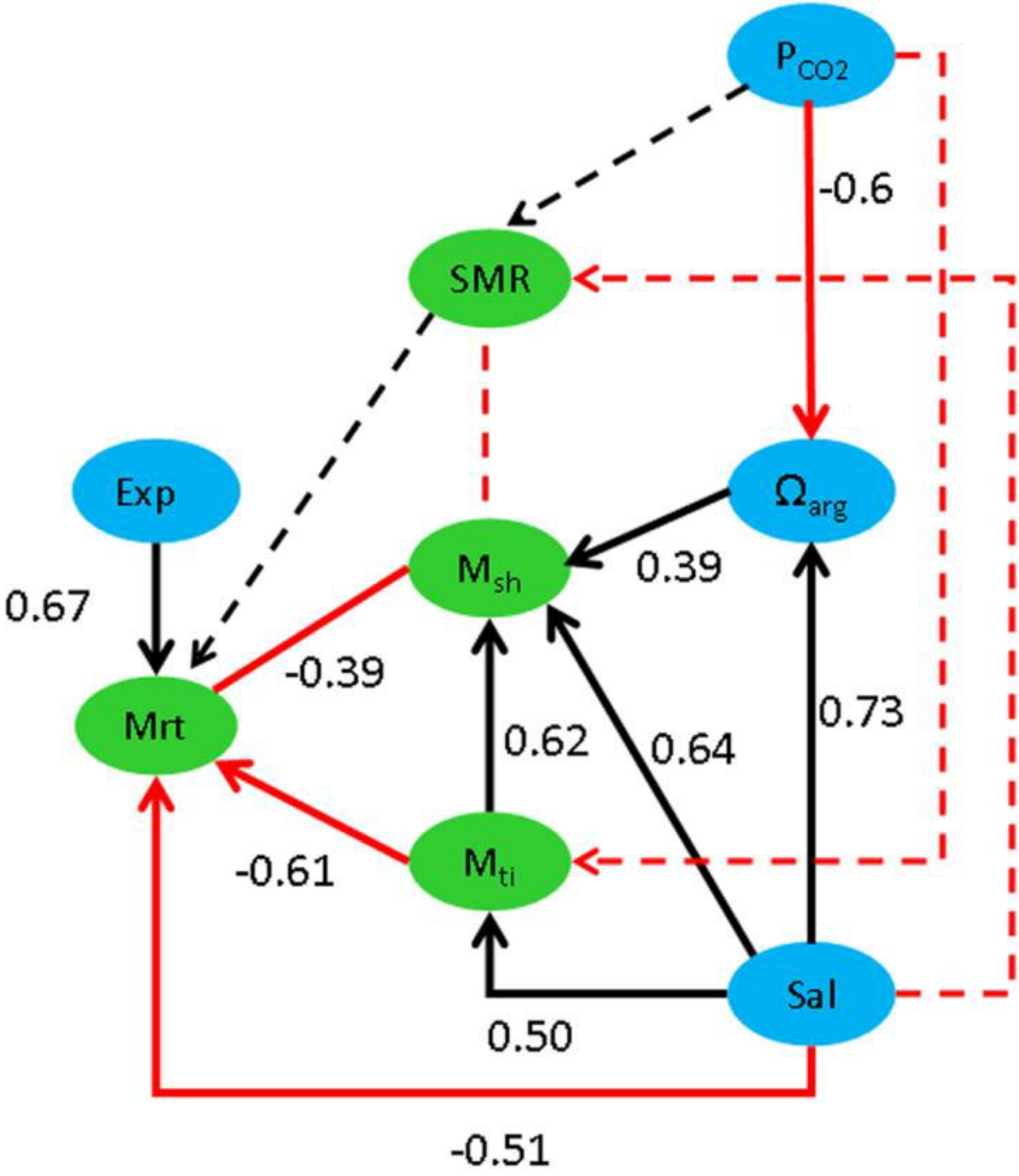
P_{CO2}
-0.6
SMR
Exp
Ω_{arg}
M_{sh}
0.39
0.67
-0.39
Mrt
0.62
0.64
0.73
-0.61
M_{ti}
Sal
0.50
-0.51

Table 1. Summary of water chemistry parameters during experimental exposures.

Salinity, temperature, pH, and TA were determined in samples from experimental tanks as described in Materials and Methods. Other parameters were calculated using co2SYS software. Data are presented as means±S.D. N=45-51 for temperature, salinity and pH, and N=5-8 for all other factors.

	Exposure salinity					
	16			32		
	~395 µatm	~800 µatm	~1500 µatm	~395 µatm	~800 µatm	~1500 µatm
pH	8.25 ±0.26	8.16 ±0.14	7.77 ±0.11	8.26 ±0.08	8.15 ±0.10	7.74 ±0.18
Temperature (°C)	19.3 ±1.6	20.4 ±0.9	19.7 ±0.8	20.1 ±1.0	20.8 ±0.8	20.4 ±0.6
Salinity	17.0 ±1.0	16.3 ±0.9	16.5 ±0.8	32.7 ±1.6	31.6 ±1.1	31.5 ±1.0
P_{CO2} (µatm)	289.1 ±30.2	704.5 ±263.5	1277.2 ±235.2	385.1 ±103.6	656.6 ±212.7	1712.6 ±346.9
TA (µmol kg^{-1} SW)	1564.9 ±86.8	1502.0 ±56.46	1518.4 ±82.69	3025.7 ±178.5	2944.6 ±113.4	2913.9 ±106.38
CO_3^{2-} (µmol kg^{-1} SW)	94.2 ±11.2	47.11 ±19.27	25.9 ±6.0	306.4 ±41.2	206.9 ±37.0	91.9 ±15.3
Ω_{Ca}	2.56 ±0.29	1.29 ±0.52	0.71 ±0.16	7.46 ±1.01	5.07 ±0.90	2.26 ±0.37
Ω_{Arg}	1.54 ±0.18	0.77 ±0.32	0.42 ±0.10	4.83 ±0.65	3.28 ±0.58	1.46 ±0.24

Table 2. ANOVA: Effects of exposure P_{CO2}, salinity, and their interaction on shell and physiological properties in juvenile *M. mercenaria*.

F-values are provided with degrees of freedom for the factor and the error in subscript. Significant p-values are in bold.

Parameters	P_{CO2}	Salinity	P_{CO2} x Salinity
Shell mass, 16 weeks	$\mathbf{F_{2,119} = 37.8}$ **p < 0.001**	$\mathbf{F_{1,119} = 8.00}$ **p < 0.001**	$F_{2,119} = 0.68$ p = 0.507
Shell mass, 21 weeks	$\mathbf{F_{2,163} = 11.2}$ **p = 0.001**	$\mathbf{F_{1,163} = 3.30}$ **p = 0.039**	$\mathbf{F_{2,163} = 13.2}$ **p < 0.001**
Tissue mass, 16 weeks	$F_{2,117} = 0.42$ p = 0.653	$\mathbf{F_{1,117} = 63.4}$ **p < 0.001**	$F_{2,117} = 1.44$ p = 0.242
Tissue mass, 21 weeks	$F_{2,147} = 2.41$ p = 0.093	$\mathbf{F_{1,147} = 51.8}$ **p < 0.001**	$\mathbf{F_{2,147} = 53.9}$ **p < 0.001**
Vickers microhardness	$\mathbf{F_{2,36} = 6.16}$ **p = 0.005**	$F_{1,36} = 2.86$ p = 0.099	$F_{2,36} = 0.77$ p = 0.472
Fracture toughness	$F_{2,33} = 0.92$ p = 0.408	$F_{1,33} = 4.00$ p = 0.054	$\mathbf{F_{2,33} = 3.75}$ **p = 0.034**
Standard metabolic rate (SMR)	$F_{2,427} = 0.36$ p =0.701	$\mathbf{F_{1,427} = 37.19}$ **p < 0.0001**	$\mathbf{F_{2,427} = 12.93}$ **p < 0.0001**